AD-A131 600 SOLUTIONS OF A FOURTH ORDER DIFFERENTIAL EQUATION DESCRIBING MODE CONVERS..(U) CALIFORNIA UNIV LOS ANGELES CENTER FOR PLASMA PHYSICS AND FUS.. 1/1

UNCLASSIFIED J E AAGGS ET AL. JUN 83 PPG-722 F/G 12/1 NL

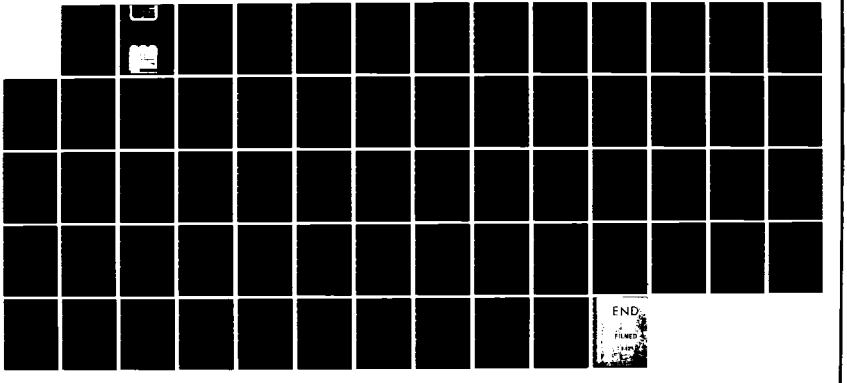

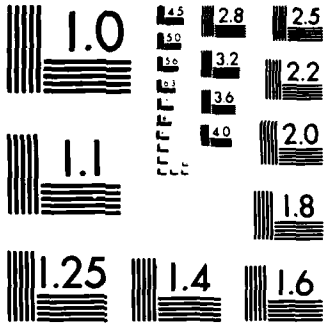

SOLUTIONS OF A FOURTH ORDER DIFFERENTIAL EQUATION DESCRIBING MODE CONVERSION IN A MAGNETIZED PLASMA

by

J.E. Maggs, Alfredo Baños, Jr.,

and G.J. Morales

Contract N00014-80-C-0373

PPG-722

June, 1983

CENTER FOR
PLASMA PHYSICS
AND
FUSION ENGINEERING

UNIVERSITY OF CALIFORNIA
LOS ANGELES

SOLUTIONS OF A FOURTH ORDER DIFFERENTIAL EQUATION DESCRIBING MODE CONVERSION IN A MAGNETIZED PLASMA

by

J.E. Maggs, Alfredo Baños, Jr.,
and G.J. Morales

Contract N00014-80-C-0373

PPG-722 June, 1983

SOLUTIONS OF A FOURTH ORDER DIFFERENTIAL EQUATION DESCRIBING MODE CONVERSION IN A MAGNETIZED PLASMA

by

J.E. Maggs

I.G.P.P., UCLA, Los Angeles, CA 90024

and

Alfredo Baños, Jr. and G.J. Morales

Physics Dept., UCLA, Los Angeles, CA 90024

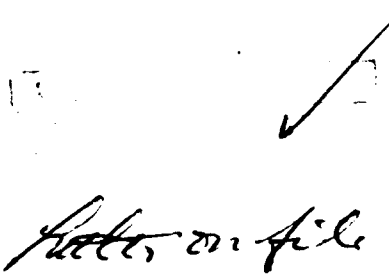

Abstract

Solutions of the equation $\varepsilon^2 u^{(4)} + z u^{(2)} + \alpha u^{(1)} + \beta_1 u - \beta_2{}^2 z u = 0$, where α, β_1, $\beta_2{}^2$ are constants, $\varepsilon^2 << 1$, and z is the independent variable are obtained using the Laplace integral technique. This equation describes the propagation of high frequency electrostatic waves near plasma resonance in a magnetized plasma with a longitudinal density gradient and is a generalization of an equation studied by Wasow and by Rabenstein in the context of boundary layer phenomena. The solutions of this fourth order equation in which the associated second order equation (i.e., $\varepsilon^2 = 0$) exhibits both a singularity (at $z = 0$) and a turning point (at $z = \beta_1/\beta_2{}^2$) fall readily into two classes. One class resembles Airy functions and exists only for ε^2 not equal to zero. In the other class, the solutions are related to confluent hypergeometric functions and can be viewed as solutions of the second order equation with small corrections proportional to ε^2. Using the integral representations of solutions it is demonstrated that each class of solutions can generate the other when the independent variable crosses the singular point. This is the physical phenomenon of mode conversion. Asymptotic descriptions of both classes of solutions are given and the form of the solutions near the singular point is expressed as a power series.

PACS number: 52.35.Fp

1. Introduction

This paper investigates the solutions of a fourth order differential equation which arises in the description of high frequency electrostatic waves near plasma resonance in a magnetized plasma with a zero order density gradient along the magnetic field. The behavior of the electrostatic potential is described by Poisson's equation which can be written as

$$\underline{\nabla} \cdot \underline{\underline{\kappa}} \cdot \underline{\nabla}\phi = i(\omega/c)\, \underline{\nabla} \cdot \underline{\underline{\kappa}} \cdot \underline{A} \,, \tag{1.1}$$

where $\underline{\underline{\kappa}}$ is the plasma dielectric tensor, ϕ the electric potential, $\underline{A}$ the vector potential, ω the angular frequency of oscillation and c the speed of light. A harmonic time dependence of the form $\exp(-i\omega t)$ is assumed. In (1.1) the term containing the vector potential can be viewed as a driving source term, which can be physically identified with an externally launched electromagnetic wave, as might be the case in a laboratory or ionospheric experiment. From this point of view (1.1) can be solved for interesting physical applications by obtaining the appropriate Green's function, a task which requires knowledge of the solutions of the associated homogeneous equation

$$\underline{\nabla} \cdot \underline{\underline{\kappa}} \cdot \underline{\nabla}\phi = 0 \,. \tag{1.2}$$

When thermal corrections associated with the motion of plasma along the magnetic field are retained, the plasma dielectric tensor becomes a second order differential operator and (1.2) can be written in dimensionless form as[1]

$$\varepsilon^2 u^{(4)} + z u^{(2)} + \alpha u^{(1)} + \beta_1 u - \beta_2{}^2 z u = 0 \,. \tag{1.3}$$

To obtain (1.3) it is assumed that the plasma has a linear density gradient with scale length L along the magnetic field direction. This assumption is appropriate for many physical applications and retains the important physical processes. In (1.3) u is the electric potential suitably normalized, and z is the distance along the magnetic field normalized to the density scale length L. The small parameter

$$\varepsilon^2 = (k_D L)^{-2} , \tag{1.4}$$

in which k_D is the Debye wave number. For typical ionospheric plasmas the parameter ε^2 can be less than 10^{-6}. The other parameters in the plasma have the values

$$\alpha = 1 ; \tag{1.5}$$

$$\beta_1 = (k_\perp L)^2 \Omega_e^2 / (\omega^2 - \Omega_e^2) ; \tag{1.6}$$

$$\beta_2^2 = (\omega/\Omega_e)^2 \beta_1 , \tag{1.7}$$

where Ω_e is the electron cyclotron angular frequency and $k_\perp$ is the fixed wave number perpendicular to the magnetic field. In obtaining solutions of (1.3) we do not restrict ourselves to the parameter values given in (1.5)-(1.7). We do, however, assume that all parameters are real and that ε^2, β_1 and β_2 are positive. These assumptions apply to a plasma in which the wave frequency is larger than the electron gyrofrequency (i.e., $\omega > \Omega_e$).

Equation (1.3) supports two distinct classes of solutions: thermal modes and cold modes. The first of these classes represents short wavelength modes in the sense that these solutions exist only when ε^2 (and hence k_D^{-2}) is not zero. The prototype equation for this class is obtained from (1.3) by setting β_1 and β_2^2 equal to zero,

$$\varepsilon^2 u^{(4)} + z u^{(2)} + \alpha u^{(1)} = 0 \ . \tag{1.8}$$

Equation (1.8) approximates (1.3) whenever the term $\varepsilon^2 u^{(4)}$ is large in comparison with $(\beta_1 u - \beta_2^2 z u)$. In this situation the solutions of (1.3) can be obtained from the solutions of (1.8) by adding corrections proportional to β_1 and β_2^2. In the WKB sense the thermal class solutions are short wavelength because the term $\varepsilon^2 u^{(4)}$ in (1.3) can be large in comparison with $\beta_1 u$ and $\beta_2^2 z u$. As shown in Sec. 3, the solutions of (1.8) are related to Airy functions since they are proportional to the $(\alpha - 2)$ derivative of Airy functions of negative argument when α is an integer.

The second class of solutions associated with (1.3) is comprised of cold plasma modes in the sense that these solutions exist even when ε^2 (and hence k_D^{-2}) is equal to zero. The prototype equation for the cold mode class is obtained from (1.3) by setting $\varepsilon^2 = 0$,

$$z u^{(2)} + \alpha u^{(1)} + \beta_1 u - \beta_2^2 z u = 0 \ . \tag{1.9}$$

The solutions of (1.9) are related to confluent hypergeometric functions. When the term $\varepsilon^2 u^{(4)}$ is small, solutions of (1.3) can be obtained from solutions of (1.9) by adding small corrections proportional to ε^2. In the WKB sense the

solutions in the cold mode class are long wavelength in that $\epsilon^4 u^{(4)}$ is small in comparison with the other terms in (1.3)

Solutions in the two classes are generally distinguished by the disparity in their wavelengths. However, near plasma resonance ($z = 0$), the WKB wavelengths of the two modes become comparable and mode conversion occurs. That is, solutions of one class generate solutions of the other class. This mode conversion process is clearly exhibited by solutions obtained in this study.

The second order equation (1.9) obtained from (1.3) by setting $\epsilon^2 = 0$ exhibits both a singularity at $z = 0$ and a turning point at $z = \beta_1/\beta_2{}^2$. The existence of the turning point distinguishes (1.3) from an equation previously studied by Wasow[2] and by Rabenstein.[3] The results obtained by these authors can be recovered in the limit $\beta_2 \to 0$. In the plasma application the singularity corresponds to plasma resonance and the turning point to upper hybrid resonance. As shown in Sec. 5 the existence of the turning point profoundly affects the structure of the cold plasma modes and allows for the existence of solutions which exhibit no mode conversion for certain restricted parameter values.

The paper is organized as follows. In Sec. 2 we introduce integral representations for the solutions of (1.3) and describe the contours associated with the solution set. In Sec. 3 the solutions corresponding to the thermal modes are obtained. In Sec. 4 expressions for the solutions corresponding to the cold plasma modes are derived. In Sec. 5, the mode conversion process and the linear independence of the solutions is discussed. Finally, in Sec. 6 the principal findings are summarized.

2. General Properties of Solutions

Since all of the coefficients of u, and its derivatives in (1.3) are linear in the independent variable z, general solutions may be found in the form of Laplace integrals. Following Coddington and Levinson,[4] but using the kernel exp(-sz) in the Laplace integral instead of exp(sz), we obtain solutions of (1.3) in the form

$$u(\alpha,\beta_1,\beta_2,\varepsilon^2,z) = \int_C \{e^{-sz}/P(s)\}\exp[-\int^s \{Q(t)/P(t)\}dt]ds \ , \tag{2.1}$$

where

$$P(t) = t^2 - \beta_2{}^2 \ ; \tag{2.2}$$

$$Q(t) = \varepsilon^2 t^4 - \alpha t + \beta_1 \ . \tag{2.3}$$

The contours C in (2.1) are chosen such that, at the endpoints of the contours, the following condition is satisfied

$$e^{-sz} \exp[-\int^s \{Q(t)/P(t)\}dt] = 0 \ . \tag{2.4}$$

Using (2.2) and (2.3) we obtain

$$\int^s (Q/P)dt = \int^s \left[\frac{\varepsilon^2 t^4 - \alpha t + \beta_1}{t^2 - \beta_2{}^2}\right] dt$$

$$= \varepsilon^2(s^3/3 + \beta_2{}^2 s) - (\alpha/2)\ell n(s^2 - \beta_2{}^2)$$

$$+ \beta\ \ell n[(s - \beta_2)/(s + \beta_2)] \ , \tag{2.5}$$

where

$$\beta = (\epsilon^2\beta_2{}^3 + \beta_1/\beta_2)/2 \ . \tag{2.6}$$

Inserting (2.5) into (2.1) the solutions can be written as

$$u = \int_C (s + \beta_2)^{\alpha_+} (s - \beta_2)^{\alpha_-} \exp[-\epsilon^2 s^3/3 - s\tilde{z}]\, ds \tag{2.7}$$

where

$$\tilde{z} = z + \epsilon^2\beta_2{}^2 \ , \tag{2.8}$$

$$\alpha_+ = \alpha/2 - 1 + \beta \ , \tag{2.9}$$

$$\alpha_- = \alpha/2 - 1 - \beta \ . \tag{2.10}$$

The endpoints of the contours C are chosen to satisfy the condition

$$(s + \beta_2)^{\alpha/2 + \beta}(s - \beta_2)^{\alpha/2 - \beta}\exp[-\epsilon^2 s^3/3 - s\tilde{z}] = 0 \ . \tag{2.11}$$

It is worth noting that the basic equation (1.3) is invariant under the transformation

$$(\alpha, \beta_1, \beta_2, \epsilon^2, z) \to (\alpha, -\beta_1, \beta_2, -\epsilon^2, -z) \ . \tag{2.12}$$

Thus another family of solutions of (1.3) is given by

$$\phi(\alpha, \beta_1, \beta_2, \epsilon^2, z) = u(\alpha, -\beta_1, \beta_2, -\epsilon^2, -z)$$

$$= \int_{C'} (s + \beta_2)^{\alpha_-}(s - \beta_2)^{\alpha_+} \exp[\epsilon^2 s^3/3 + s\tilde{z}]\, ds \ , \tag{2.13}$$

where the endpoints of the contours C' satisfy the condition

$$(s + \beta_2)^{\alpha/2 - \beta}(s - \beta_2)^{\alpha/2 + \beta}\exp[\epsilon^2 s^3/3 + s\tilde{z}] = 0 \ . \tag{2.14}$$

In the following we investigate the functions u as defined by (2.7) in detail and use the transformation (2.12) to obtain the functions ϕ.

The condition (2.11) that must be met at the endpoints of the contours can be satisfied at large s by choosing the real part of $\varepsilon^2 s^3/3$ to be positive. Since we have chosen ε^2 real, this requirement becomes, with j = 1,2,3,

$$2\pi(2-j)/3 - \pi/6 < \arg s < \pi/6 + 2\pi(2-j)/3 \ . \tag{2.15}$$

Thus as shown in Figure 1, there are three open sectors in the s-plane of angular width $\pi/3$ centered about $2\pi/3$, 0, and $-2\pi/3$ in which the contour may go to infinity and satisfy the condition (2.11). Since we have stipulated that α, β_1, β_2 and ε^2 are real and positive, the quantity $\alpha/2 + \beta$ is real and positive. Thus the condition (2.11) can also be satisfied at the point $s = -\beta_2$ because the quantity $(s + \beta_2)^{\alpha/2+\beta}$ is then always zero. Since the quantities α_+ and α_-, while real, are not necessarily integers, the points $s = \pm\beta_2$ are, in general, branch points. If the s-plane is cut from β_2 to positive infinity and from $-\beta_2$ to negative infinity along the real axis as shown in Figure 1, the multi-valued function $(s - \beta_2)^{\alpha_-}(s + \beta_2)^{\alpha_+}$ in the integrand of (2.7) can be written as

$$(s - \beta_2)^{\alpha_-}(s + \beta_2)^{\alpha_+} = (r_1 e^{i\theta_1})^{\alpha_-}(r_2 e^{i\theta_2})^{\alpha_+}$$

$$= \exp[\alpha_- \ell n r_1 + i\alpha_-(\theta_1 + 2\pi n) + \alpha_+ \ell n r_2 + i\alpha_+(\theta_2 + 2\pi m)] \ , \tag{2.16}$$

with $-\pi < \theta_2 < \pi$ and $0 < \theta_1 < 2\pi$. In (2.16) the various branches of the ℓn functions are represented by the integers m and n which denote various sheets of the Riemann surface. Each sheet of the Riemann surface can thus be labeled by the pair of integers (m,n). The s-plane represented in Figure 1 corresponds to the principal branches of the ℓn functions m=n=0 and is labeled by (0,0).

The endpoints for contours corresponding to solutions of (1.3) must be chosen to satisfy the relation given in (2.11). This condition can be met by choosing the contours that begin and end at infinity in any of the sectors $j = 1,2,3$ or contours that begin at the branch point $s = -\beta_2$ and end at $s = -\beta_2$ or, alternatively, proceed to infinity within the numbered sectors. Contours which correspond to solutions in the thermal mode class are shown in Figure 2. These contours begin at infinity in one sector and end at infinity in another sector. The solutions obtained from (2.7) by integrating along these contours are labeled A_j where j refers to the sector opposite the contour. For example, the contour beginning in sector 2 and ending in sector 1 corresponds to the solution labeled A_3. The contour for the solution A_2 begins in sector 1 and crosses the branch cut along the negative real axis before proceeding to infinity in sector 3. This part of the contour for the solution A_2 lies in the (1,0) Riemann sheet (i.e., the sheet with m = 1, n = 0) and is thus shown as a broken line in Fig. 2.

Contours corresponding to solutions in the cold plasma mode class have at least one end point at $s = -\beta_2$ and are shown in Figs. 3(a) and 3(b). The contour corresponding to the solution labeled B_0 starts at the point $s = -\beta_2$, encircles the point $s = \beta_2$ in the counter-clockwise direction and ends again at $s = -\beta_2$. The contour for B_0 crosses the branch line along the positive real axis and thus crosses onto the (0,1) Riemann sheet (i.e., m = 0, n= 1). The portion of the contour lying in the (0,1) sheet is shown as a dashed line. Contours corresponding to solutions labeled B_j where j corresponds to the sector in which they proceed to infinity are illustrated in Figure 3(a). These contours start at the point $s = -\beta_2$ and proceed to infinity in sector j in such a fashion that the radius vector from $s = \beta_2$ to a point on the contour moves in the

clockwise direction as the point proceeds to infinity. Thus the contour for the solution B_2 passes above the point $s = \beta_2$. Contours for solutions labeled B_j are shown in Figure 3(b). These contours also start at $s = -\beta_2$ but the radius vector from $s = -\beta_2$ to a point on the contour moves in the counter-clockwise direction as the point proceeds to infinity in sector j. Thus the contour for $\tilde{B}_2$ passes below the point $s = \beta_2$. Note that the contour for $\tilde{B}_1$ shown in Figure 3(b) crosses the branch cut along the positive real axis and thus passes onto the (0,1) Riemann sheet. The portion of the contour on the (0,1) sheet is again shown as a dashed line. While not illustrated in Figure 3(a), the contour for the solution B_3 would similarly cross the branch cut along the positive real axis but in a clockwise direction and thus would pass onto the (0,-1) Riemann sheet. The contours for the solutions B_j and $\tilde{B}_j$ (j = 1,2,3) proceed to infinity along the same asymptotic direction in sector j.

Although illustrated only for the principal sheet, the contours corresponding to solutions B_j, $\tilde{B}_j$, B_0 and A_j may begin on any sheet of the Riemann surface. In order to distinguish among functions corresponding to contours on different sheets of the Riemann surface we introduce the notation X(m,n;p), where X is any of the solutions A_j, B_0, B_j, $\tilde{B}_j$, m and n are integers specifying the sheet, and p denotes dependence on the parameters α, β_1, β_2, ε^2, z. In this notation the values m and n indicate the sheet on which the contour begins. As described above some contours begin on one sheet and end on an adjacent sheet. Thus $A_2(0,0;p)$ indicates the contour beginning in the sheet with m=0, n=0 but, as shown in Fig. 2, it ends in the sheet with m=1, n=0. For brevity of notation we omit the dependence on m and n or other parameters unless they are needed to clarify the discussion. Furthermore, if the values of m and n are not explicitly indicated the principal values m=0, n=0 are to be assumed. As an illustration

we have drawn in Figure 3(a) the contour corresponding to the function $B_3(0,1)$. The contour begins on the sheet (0,1) (and is thus shown dashed) and passes onto the principal sheet when it crosses the branch cut extending from β_2 to positive infinity. Finally, functions corresponding to contours on different sheets are simply related. Employing the notation described above and using (2.16) one can write

$$X(m,n) = e^{i2\pi m\alpha_+} e^{i2\pi n\alpha_-} X(0,0) \ . \tag{2.17}$$

Since the integrand in (2.7) is analytic throughout the entire s-plane except at the points $s = \pm\beta_2$, Cauchy's theorem can be used to establish relationships among the various solutions A_j, B_0, B_j, and $\tilde{B}_j$ by using combinations of the appropriate contours. In order to facilitate the derivation of relations among the solutions all of the contours in Figs. 2 and 3 have been combined into Fig. 4. Refering to Fig. 4 and using Cauchy's theorem the following relationships can be established

$$B_2 = B_1 - A_3 \tag{2.18}$$

$$\tilde{B}_1 = \tilde{B}_2 + A_3(0,1) \tag{2.19}$$

$$B_1 = \tilde{B}_3(1,0) - A_2 \tag{2.20}$$

$$B_3(0,1) = B_2(0,1) - A_1 \tag{2.21}$$

$$\tilde{B}_3 = \tilde{B}_2 - A_1 \tag{2.22}$$

$$\tilde{B}_j - B_j(0,1) = B_0 \ ; \quad (j = 1,2,3) \tag{2.23}$$

The relations (2.18), (2.20) and (2.22) can be readily verified by referring to Fig. 4. To verify the remaining relations it is helpful to picture the contours for $\tilde{B}_2$ or $B_2(0,1)$ as crossing the branch cut which extends from β_2 to infinity. The relations (2.18)-(2.23) prove useful in obtaining, among other things, analytic continuations of the functions B_j and $\tilde{B}_j$. Having determined the set of contours which yield solutions of (1.3) in the integral representation (2.7) we next proceed to evaluate these solutions in detail. We first examine the solutions A_j before proceeding to investigate the solutions B_0, B_j and $\tilde{B}_j$.

3. The Solutions A_j

The functions $A_j(z)$ are defined by the integral representation (2.7) in which the paths of integration are given by the contours $C(A_j)$ as illustrated in Fig. 2. In this section we first discuss the asymptotic behavior of the functions $A_j(z)$ for $|z| >> \epsilon^{2/3}$ and then derive a power series expansion which is particularly useful for small argument, $z \to 0$. In both cases it is convenient to introduce the transformation

$$\sigma = \epsilon^{2/3}s; \quad \eta = \epsilon^{-2/3}\tilde{z}; \quad \sigma_o = \sigma(\beta_2) = \epsilon^{2/3}\beta_2 \quad , \tag{3.1}$$

where $\tilde{z} = z + \epsilon^2\beta_2^2 \simeq z$ when $\epsilon^2 << 1$. Making use of (3.1) in (2.7) we obtain the integral representation

$$A_j(\eta) = \epsilon^{-2(\alpha-1)/3} \int_{C'(A_j)} (\sigma - \sigma_o)^{\alpha-} (\sigma + \sigma_o)^{\alpha+} \exp[-(\sigma^3/3 + \sigma\eta)]\, d\sigma \ , \tag{3.2}$$

where $C'(A_j)$ is the image of the contour $C(A_j)$ under the transformation (3.1)

To evaluate (3.2) asymptotically we employ the saddle point method of integration.[5] We note that the derivative of the exponent $f(\sigma) = -(\sigma^3/3 + \sigma\eta)$, namely $f'(\sigma) = -(\sigma^2 + \eta)$, when equated to zero yields two roots, or saddle points, at $\sigma_s = \pm i\eta^{\frac{1}{2}}$. For our purpose we discard the minus sign and choose the saddle point

$$\sigma_s = i\eta^{\frac{1}{2}}; \quad \eta = |\eta|e^{i\theta}; \quad |\eta| >> 1 \quad , \tag{3.3}$$

from which we deduce that, when $\theta = 0$, $\sigma_s = i\eta^{\frac{1}{2}}$ with η real and positive; when $\theta = \pi$, $\sigma_s = e^{i\pi} |\eta|^{\frac{1}{2}} = -(-\eta)^{\frac{1}{2}}$ with η real and negative, and finally, when $\theta = 2\pi$, $\sigma_s = e^{3\pi i/2} |\eta|^{\frac{1}{2}} = -i\eta^{\frac{1}{2}}$, with η again real and positive. These values of σ_s represent the principal saddle points and their location in the σ-plane is illustrated in Fig. 5. The principal saddle points at $\theta = 0$, π and 2π correspond respectively to the contours for A_3, A_2, and A_1. The other choice of sign, $\sigma_s = -i\eta^{\frac{1}{2}}$, yields nothing new.

The contours $C'(A_j)$ in (3.2), as shown in Fig. 5, are asymptotic to the rays with phase 0, $2\pi/3$, and $4\pi/3$. Accordingly, making use of (3.3) one has the following argument ranges

$$2\pi(2-j)/3 + 2\pi/3 < \arg \sigma_s < 4\pi/3 + 2\pi(2-j)/3;$$

$$4\pi(2-j)/3 + \pi/3 < \theta < 5\pi/3 + 4\pi(2-j)/3 \ . \tag{3.4}$$

As shown in Fig. 5, we can use (3.4) to trace the path of the saddle point with $|\eta|$ fixed as θ varies from $-\pi$ to 3π, or arg σ_s varies from 0 to 2π. It is seen from Fig. 5 that the chosen saddle point σ_s in (3.3) corresponds to the functions A_3, A_2, and A_1 and traces a circle of radius $\sigma = |\eta|^{\frac{1}{2}}$. However, we note that σ_s starts just above the right hand branch cut of Fig. 1 and traces a semi-circle in the upper half of the σ-plane, at which point σ_s crosses the left-hand branch cut from the principal sheet onto the adjacent sheet of the Riemann surface, $m = 1$, $n = 0$ in accordance with (2.16), and traces a semi-circle on the lower half of the $(1,0)$ sheet.

We observe from (3.4) that the path of steepest descents for A_3 lies entirely on the principal sheet of the Riemann surface and therefore the saddle point integration of (3.2) is independent of the branch cuts, which is to say that the multivalued factors $(\sigma - \sigma_o)^{\alpha_-}$ and $(\sigma + \sigma_o)^{\alpha_+}$ in the integrand of (3.2)

are assigned their principal values. For A_2 the path of steepest descents starts at infinity on the principal sheet and terminates at infinity on the adjacent m = 1, n = 0 sheet thus crossing the left-hand branch cut. However, since the saddle point also crosses onto the (1,0) sheet, the saddle point integration is carried out assuming that the multivalued factors in (3.2) vary continuously as the saddle point crosses the branch cut. Finally, as regards the path of steepest descents for A_1, we note that it is also independent of the branch cuts but now lies entirely on the m = 1, n = 0 sheet and, therefore, the saddle point integration of (3.2) evaluates $A_1(1,0)$. The multivalued factor is evaluated according to (2.16) with m = 1, n = 0.

Next, we wish to determine the direction of traversal through the chosen saddle point σ_s. In the vicinity of σ_s we can write $-x^2 = \frac{1}{2} f''(\sigma_s)(\sigma - \sigma_s)^2 + \ldots$, where x is real and positive ($x > 0$) after passing through the saddle point. In the present instance $-\frac{1}{2} f''(\sigma_s) = \sigma_s = i\eta^{\frac{1}{2}}$. Hence, extracting the square root and putting $w = \sigma - \sigma_s$, we have $x = \pm[-\frac{1}{2} f''(\sigma_s)]^{\frac{1}{2}} w = \pm(\sigma_s)^{\frac{1}{2}} w$. Ignoring the plus sign, writing $-1 = e^{-i\pi}$ and putting arg x = 0 yields

$$\arg w = \pi - \arg (\sigma_s)^{\frac{1}{2}} = 3\pi/4 - \theta/4 \quad , \tag{3.5}$$

which says that, for A_3 and $\theta = 0$, arg $w = 3\pi/4$; for A_2 and $\theta = \pi$, arg $w = \pi/2$, and for A_1 and $\theta = 2\pi$, arg $w = \pi/4$. We note that (3.5) gives, for A_3 and A_1, the correct direction of traversal through the saddle point in accordance with the arrows drawn in Figs. 2 and 5. However, for A_2 the direction of traversal is opposite to the direction of the arrow, which gives a minus sign to be attached to the final result for A_2.

Asymptotically, $|z| >> \varepsilon^{2/3}$ and with $\varepsilon^2 << 1$ yields $\tilde{z} = z + \varepsilon^2\beta_2 \simeq z$ and $\eta \simeq \varepsilon^{-2/3}z$. Furthermore, from (2.6) $\beta = \varepsilon^2\beta_2^3/2 + \beta_1/2\beta_2 \simeq \beta_1/2\beta_2 \equiv \beta_o$, from which instead of the exponents α_+ and α_- defined by (2.9) and (2.10) we introduce

$$a_+ = \alpha/2 - 1 + \beta_o \; ; \; a_- = \alpha/2 - 1 - \beta_o \; . \tag{3.6}$$

After this preamble, we can now apply the familiar leading term formula of the method of steepest descents to compute an asymptotic representation for the functions $A_j(\eta)$ given by the integral representations (3.2). Thus we obtain, for the saddle point $\sigma_s = i\eta^{1/2}$ and $j = 1,2,3$, the leading terms:

$$A_j(\bar{\gamma},0;\eta) \sim \sqrt{\pi}\,(-)^j\varepsilon^{-2(\alpha-1)/3}(\sigma_s - \sigma_o)^{a_-}(\sigma_s + \sigma_o)^{a_+}\frac{\exp[f(\sigma_s)]}{[-f''(\sigma_s)/2]^{1/2}}\{1+O(\sigma_s^{-3})\}$$

$$= \sqrt{\pi}\,(-)^j\varepsilon^{-2(\alpha-1)/3}(i\eta^{1/2}-\sigma_o)^{a_-}(i\eta^{1/2}+\sigma_o)^{a_+}\frac{e^{-i\zeta}}{[i\eta^{1/2}]^{1/2}}\{1+O(1/\zeta)\} \tag{3.7}$$

where

$$\zeta \equiv (2/3)\eta^{3/2} = (2/3)\varepsilon^{-1}z^{3/2} \; ; \; \bar{\gamma} = \tfrac{1}{2}[1 - (-)^j]\gamma \; , \tag{3.8}$$

and

$$\gamma \equiv \begin{cases} 0 & \mathrm{Im}(\sigma_s) > 0 \\ 1 & \mathrm{Im}(\sigma_s) \leq 0 \end{cases} \tag{3.9}$$

We have introduced the factor $\bar{\gamma}$ to insure the continuity of the function A_2 as the saddle point crosses the branch cut along the negative real axis. The general solution $A_j(m,n;\eta)$ can be found from (3.7) by using (2.17).

From (3.8) we deduce that for $j = 3$ and $\theta = 0$, $-i\zeta = -(2/3)i\eta^{3/2}$ with η real and positive; for $j = 2$ and $\theta = \pi$, $-i\zeta = -(2/3)(-\eta)^{3/2}$ with η real and negative, and finally, for $j = 1$ and $\theta = 2\pi$, $-i\zeta = (2/3)i\eta^{3/2}$ with η again real and positive. Finally, to conclude our asymptotic leading term presentation we translate (3.7) into a function of z. Recalling that $\sigma_o = \varepsilon^{2/3}\beta_2$, we obtain, after some algebraic manipulations,

$$A_j(\bar{\gamma},0;z) = (-)^j(iz^{1/2}/\varepsilon-\beta_2)^{a_-}(iz^{1/2}/\varepsilon+\beta_2)^{a_+}\frac{\sqrt{\pi}\,e^{-i\zeta}}{[i\varepsilon z^{1/2}]^{1/2}}\{1+O(1/\zeta)\}\,, \tag{3.10}$$

where the multivalued factor is evaluated as discussed above.

In (3.7) we have retained the term σ_o even though we have assumed $|\sigma_s| >> \sigma_o$ (i.e., $|z| >> \varepsilon^2\beta_2^2$) in order to preserve the topological structure of the cut σ-plane. It is useful to obtain a form for A_j in which σ_o is ignored in comparison with σ_s but this procedure will alter the topology of the cut σ-plane. Ignoring the σ_o term in (3.7) is formally equivalent to setting $\sigma_o = 0$ so that there is a single branch point at the origin rather than two branch points. The multivalued factor in (3.7) becomes $\sigma_s^{a_-}\sigma_s^{a_+} = \sigma_s^{\alpha-2}$. Taking the branch cut to lie along the positive real axis and the principal sheet to have argument range $0 < \arg\sigma_s < 2\pi$, we see that the argument range for the multivalued factor $(\sigma_s - \sigma_o)^{a_-}(\sigma_s + \sigma_o)^{a_+}$ in (3.7) exactly coincides with that of $\sigma_s^{a_-}\sigma_s^{a_+}$ when $\sigma_o=0$. Noting from (2.17) that $A_1(1,0;\eta) = e^{i2\pi\alpha_+}A_1(\eta)$ we can then write

$$A_j(\eta) \sim (-)^j \sqrt{\pi}\, p_j\, \varepsilon^{-2(\alpha-1)/3} (i\eta^{1/2})^{\alpha-5/2} e^{-i\zeta} \quad , \tag{3.11}$$

where the phase factors p_j are:

$$p_3 = p_2 = 1 \; ; \; p_1 = e^{-i2\pi\alpha_+} \quad . \tag{3.12}$$

In (3.11) the argument range of $(i\eta^{1/2})$ is from 0 to 2π.

As mentioned previously the functions $A_j(\eta)$ are closely related to Airy functions. This relationship is best elucidated if we consider the case $\sigma_o = 0$, which is equivalent to setting $\beta_2 = \beta_1 = 0$, with the result that (1.3) reduces to (1.8). Putting $\eta = \varepsilon^{2/3} z$ in accordance with (3.1) and writing $\chi(\eta)$ instead of $u(z)$, we obtain from (1.8) the equation $\chi^{(3)} + \eta\chi^{(1)} + (\alpha - 1)\chi = 0$. When α is an integer, it can be shown that $\chi(\eta)$ is proportional to the $(\alpha - 2)$ derivative of any Airy function of negative argument, i.e., any solution of $v^{(2)} + \eta v = 0$. When $(\alpha - 2)$ is a negative integer the above statement must be interpreted as the $|\alpha - 2|$ integral of $v(\eta)$. The same conclusions follow from the integral representation (3.2) upon setting $\sigma_o = 0$; that is, $A_j(\eta)$ in (3.11), when α is an integer, is proportional to the $(\alpha - 2)$ derivative of the asymptotic leading term of an Airy function of negative argument, and hence is a solution of our basic equation (1.3).

We now proceed to discuss the small argument behavior of the function $A_j(\eta)$. For this purpose we make use again of the scale transformation (3.1) and the integral representation (3.2) wherein α_+ and α_- have their original definitions (2.9) and (2.10). To evaluate (3.2) we first construct the power series expansion

$$(\sigma - \sigma_o)^{\alpha_-} (\sigma + \sigma_o)^{\alpha_+} = \sigma^{\alpha-2} \sum_{m=0}^{\infty} c_m w^m \qquad ; \qquad |w| < 1 \; , \tag{3.13}$$

where $w = \sigma_o/\sigma$ and the expansion coefficients

$$c_m = \sum_{n=0}^{\infty} (-)^n \begin{pmatrix} \alpha_- \\ n \end{pmatrix} \begin{pmatrix} \alpha_+ \\ m-n \end{pmatrix} \tag{3.14}$$

are given in terms of the familiar binomial coefficients. The expansion on the right of (3.13) is absolutely convergent for $|w|<1$ because it arises from the multiplication of the two absolutely convergent binomial expansions corresponding to the factors $(\sigma-\sigma_o)^{\alpha_-}$ and $(\sigma+\sigma_o)^{\alpha_+}$. This result follows from Cauchy's Theorem on the multiplication of absolutely convergent series.[6] Since the power series (3.13) is absolutely convergent for $|w|=1-\delta$, where δ is an arbitrarily small number, it also follows that the series in question is uniformly convergent[7] for $|w| \leq 1 - \delta$. Hence, we can replace the product $(\sigma - \sigma_o)^{\alpha_-}(\sigma + \sigma_o)^{\alpha_+}$ in the integrand of (3.2) with the uniformly convergent series (3.13) and integrate term by term to obtain, for $j = 1,2,3$,

$$A_j(\eta) = p_j \varepsilon^{-2(\alpha-1)/3} \sum_{m=0}^{\infty} c_m \sigma_o^m \, g_j(\eta,\alpha-m) \tag{3.15}$$

where the phase factors p_j are given by (3.12), and where

$$g_j(\eta,\alpha) = \int_{C'(A_j)} d\sigma \, \sigma^{\alpha-2} \, e^{-\sigma^3/3-\sigma\eta} \tag{3.16}$$

are the same functions introduced by Rabenstein.[8] In (3.16) the contour $C'(A_j)$ is chosen such that $|\sigma| > \sigma_o$ everywhere along the contour, which is the condition for the convergence of the series (3.13).

A convenient expression for the functions $g_j(\eta,\alpha)$, $j = 1,2,3$, is obtained by expanding the factor $\exp[-\sigma\eta]$ into a power series

$$e^{-\sigma\eta} = \sum_{k=0}^{\infty} [(-)^k/k!]\sigma^k\eta^k \quad , \tag{3.17}$$

which is uniformly convergent in the finite σ plane, $|\sigma| < \infty$. Introducing (3.17) into (3.16) and integrating term by term we obtain

$$g_j(\eta,\alpha) = \sum_{k=0}^{\infty} [(-)^k/k!]\eta^k \int_{C'(A_j)} d\sigma\ \sigma^{\alpha-2+k}\ e^{-\sigma^3/3} \quad . \tag{3.18}$$

Putting $y = \sigma^3/3$, the integrals in (3.18) become

$$I_j(\alpha,k) = \int_{C'(A_j)} d\sigma\ \sigma^{\alpha-2+k}\ e^{-\sigma^3/3} = 3^{(\alpha+k-4)/3} \int_{H_j} dy\ e^{-y}\ y^{(\alpha+k-4)/3} \quad , \tag{3.19}$$

where the contour H_j is the image of $C'(A_j)$ under the transformation. To ascertain the shape of H_j consider, for example, $C'(A_3)$ which begins at infinity with $\arg\sigma = 0$ and proceeds to infinity with $\arg\sigma = 2\pi/3$. Under the transformation, $y = \sigma^3/3$, the contour H_3 begins at infinity with $\arg y = 0$, encircles the origin in the counter-clockwise direction, and proceeds to infinity with $\arg y = 2\pi$. Therefore, H_3 is simply Hankel's contour and we can write

$$I_3(\alpha,k) = 3^{(\alpha+k-4)/3} \int_{\infty}^{(0+)} dy\ e^{-y}\ y^{(\alpha+k-4)/3} \quad , \tag{3.20}$$

which can be evaluated in terms of gamma functions.

Proceeding in an entirely analogous fashion, we ascertain that the contour H_2 starts at infinity with arg y = 2π, encircles the origin, and terminates at infinity with arg y = 4π, whereas the contour H_1 begins with arg y = 4π and ends with arg y = 6π. Thus, introducing the abbreviation

$$\rho = \rho(\alpha,k) = (4-\alpha-k)/3 \quad , \tag{3.21}$$

and making use of a generalization of Hankel's integral representation,[9]

$$I_j(\alpha,k) = 2\pi i \exp[\pi i(1 - \rho)(7 - 2j)]/\{3^{\rho}\Gamma(\rho)\} \ . \tag{3.22}$$

Making use of (3.18) and (3.19) we obtain the expansion

$$g_j(\eta,\alpha) = \sum_{k=0}^{\infty} [(-)^k/k!]I_j(\alpha,k)\eta^k \quad , \tag{3.23}$$

where the functions $I_j(\alpha,k)$ are given by (3.22). Finally, using (3.15) we obtain the power series expansions

$$A_j(\eta,\alpha) = p_j \ \epsilon^{-2(\alpha-1)/3} \sum_{m=0}^{\infty} \ \sum_{k=0}^{\infty} c_m \ \sigma_o^{\,m}[(-)^k/k!]I_j(\alpha - m,k)\eta^k \quad , \tag{3.24}$$

where the p_j are the phase factors given in (3.12) These functions, for j = 1,2,3, correspond to their asymptotic counterparts $A_j(\eta)$ given by (3.7) and are subject to the same argument ranges for η as given by (3.4).

4. The Solutions B_j, $\tilde{B}_j$, and B_0

The functions B_j, $\tilde{B}_j$, and B_0 are solutions of (1.3) and are given by the integral representation (2.7), where the corresponding paths of integration are shown in Figs. 3(a) or 3(b). Since we are unable to directly evaluate these integrals, we resort to a perturbation expansion based on the fact that $\varepsilon^2 << 1$. Thus expanding (2.7) in a power series in ε^2 we show in the Appendix that, to first order in ε^2,

$$u(\alpha,\beta_1,\beta_2,\varepsilon^2;z) = u(\alpha,\beta_1,\beta_2,0;z) + \varepsilon^2(\partial_{\varepsilon^2}u)\Big|_{\varepsilon^2=0}$$

$$= u_0 - \varepsilon^2[h(u_0)/4\beta_2] \quad , \tag{4.1}$$

where $u(\alpha,\beta_1,\beta_2,\varepsilon^2;z)$ is any of the solutions B_0, B_j or $\tilde{B}_j$ and u_0 is the corresponding solution evaluated at $\varepsilon^2 = 0$. The expression for $h(u_0)$ is given in (A.2.6) in terms of u_0 evaluated at shifted values of the parameters α and β_1.

We observe that the functions $u_0(z)$ are solutions of the reduced ($\varepsilon^2 = 0$) second order differential equation (1.9) and are given by the integral representation

$$u_0(z) = \int_C (s - \beta_2)^{a_-}(s + \beta_2)^{a_+} e^{-sz}\, ds \ , \tag{4.2}$$

where a_+ and a_- are given by (3.6) in terms of α and $\beta_0 = \beta_1/2\beta_2$. The contours of integration in (4.2) are those associated with B_j, $\tilde{B}_j$, and B_0 and respectively yield functions denoted by b_j, $\tilde{b}_j$ and b_0. Finally, if we introduce the transformation $u(x) = g(x)\exp(-x/2)$ with $x = 2\beta_2 z$ into (1.9), we obtain Kummer's differential equation[10]

$$xg^{(2)} + (\alpha - x)g^{(1)} - (\alpha/2 - \beta_0)g(x) = 0 \ , \tag{4.3}$$

which has two independent solutions that, for our purpose, we write as

$$g_1(x) = M(\alpha/2 - \beta_0, \alpha; x) \ ; \tag{4.4}$$

$$g_2(x) = U(\alpha/2 - \beta_0, \alpha; x) \ , \tag{4.5}$$

where M and U are Kummer functions. Since the properties of these functions are well-known, we proceed to obtain expressions for b_j, $\tilde{b}_j$, and b_0 in terms of Kummer functions.

The function b_0 obtained from (4.2) by integrating along the contour associated with B_0 is related to the Kummer function $M(b,c;z)$. This can be demonstrated by using the transformation

$$s = 2\beta_2(t - \tfrac{1}{2}) \tag{4.6}$$

in (4.2) to obtain

$$b_0 = (2\beta_2)^{\alpha-1} e^{\beta_2 z} \int_0^{(1+)} (t - 1)^{a_-} t^{a_+} e^{-2\beta_2 zt} \, dt \ . \tag{4.7}$$

The contour in (4.7) is the image of $C(B_0)$ under the transformation (4.6). It starts at the origin, circles the point $t = 1$ in the positive direction and returns to the origin. The integrand in (4.7) is bounded everywhere along the contour for $|z| < \infty$ so that an expression can be obtained for b_0 that is valid for the entire z-plane, as is shown in the following.

The integral representation for the Kummer function M(b,c;z) for Re(b) > 0 is[11]

$$M(b,c,z) = \frac{\Gamma(c)\ \Gamma(b-c+1)}{2\pi i\ \Gamma(b)} \int_0^{(1+)} e^{zt}\ t^{b-1}(t-1)^{c-b-1}\ dt\ . \tag{4.8}$$

From (3.6) one has $a_+ = \alpha/2 + \beta_0 - 1$, where $\beta_0 = \beta_1/2\beta_2$ is β evaluated at $\epsilon^2 = 0$, and since α, β_1, β_2 are taken as real and positive, $\mathrm{Re}(\alpha/2 + \beta_0) > 0$ so that (4.8) can be used in (4.7) to obtain

$$b_0 = (2\beta_2)^{\alpha-1}\ e^{\xi/2} \left\{ \frac{2\pi i\ \Gamma(\alpha - a)}{\Gamma(\alpha)\ \Gamma(1-a)}\ M(\alpha-a,\alpha;-\xi) \right\} \tag{4.9}$$

where $a = \alpha/2 - \beta_0$ and $\xi = 2\beta_2 z$. Finally using the Kummer transformation

$$M(b,c;z) = e^{z}M(c-b,c;-z) \tag{4.10}$$

yields

$$b_0 = (2\beta_2)^{\alpha-1}\ e^{-\xi/2} \left\{ \frac{2\pi i\ \Gamma(\alpha - a)}{\Gamma(\alpha)\ \Gamma(1-a)}\ M(a,\alpha;\xi) \right\}\ . \tag{4.11}$$

An expression for B_0, accurate to order ϵ^2, can thus be obtained by combining (4.1), (4.11) and (A.2.6):

$$\begin{aligned} B_0 = (2\beta_2)^{\alpha-1}\ \frac{2\pi i\ \Gamma(\alpha - a)}{\Gamma(\alpha)\ \Gamma(1-a)}\ e^{-\xi/2} \Big\{ & [1 - (\epsilon^2\beta_2{}^4)\partial_{\beta_1}]M(a,\alpha;\xi) \\ & - (\epsilon^2/12\beta_2)[M(a+1,\alpha+4;\xi) - M(a+3,\alpha+4;\xi)] \\ & - (\epsilon^2/12\beta_2 + \epsilon^2\beta_2/4)[M(a+2,\alpha+2;\xi) - M(a,\alpha+2;\xi)] \Big\}\ . \end{aligned} \tag{4.12}$$

From (4.12), the value of B_0 can be found to order ϵ^2 for any z with $|z| < \infty$.

The solutions B_j and $\tilde{B}_j$ are related to a linear combination of the Kummer functions M(b,c;z) and U(b,c;z). The contours associated with the solutions B_j and $\tilde{B}_j$ go to infinity in the sector j in accordance with (2.15) and the integrand of u_o as given in (4.2) has the asymptotic value $s^{\alpha-2}\, e^{-zs}$. In order to insure that the integrand remains bounded for all α one must require that $|z| > |z_o| > 0$ (for some given z_o), and

$$-\pi/2 < \arg(sz) < \pi/2 \ . \tag{4.13}$$

However, the subscript j already implies an argument range for the variable of integration s along the contours associated with the solutions B_j and $\tilde{B}_j$. As given by (2.15) these ranges are, for the solutions B_j,

$$2\pi(2 - j)/3 - \pi/6 < \arg s < \pi/6 + 2\pi(2 - j)/3 \ . \tag{4.14}$$

From (4.13) and (4.14) one finds that the solutions b_j are well-defined only over certain regions of the z-plane, namely,

$$2\pi(j - 2)/3 - 2\pi/3 < \arg z < 2\pi/3 + 2\pi(j - 2)/3 \ . \tag{4.15}$$

Using (4.2) and the transformation

$$s = 2\beta_2(t + \tfrac{1}{2}) \ , \tag{4.16}$$

yields

$$b_j = (2\beta_2)^{\alpha-1}\, e^{-\xi/2} \int_{-1}^{\infty e^{i\theta}} t^{a_-}(t + 1)^{a_+}\, e^{-\xi t}\, dt \ , \tag{4.17}$$

where the angle θ lies in the sector j. The paths of integration given in (4.17) are the image of the contours corresponding to the solutions B_j under the transformation (4.16). Similarly, from the definition of the $\tilde{B}_j$ contours, we have

$$\tilde{b}_j = (2\beta_2)^{\alpha-1} e^{-\xi/2} \int_{-1}^{\infty e^{i(\theta + 2\pi)}} t^{a_-}(t + 1)^{a_+} e^{-\xi t} dt . \tag{4.18}$$

The integral representation for the Kummer function U is[12]

$$U(b,c;y) = (1/2\pi i)\Gamma(1 - b)e^{-b\pi i} \int_{\infty e^{i\theta}}^{(0+)} t^{b-1}(1 + t)^{c-b-1} e^{-yt} dt . \tag{4.19}$$

In the integral of (4.19) the contour starts at infinity with argument θ, circles the origin in the positive direction (i.e., cuts the negative t-axis) and returns to infinity with argument $\theta + 2\pi$. Since the integrand of (4.19) is analytic in the region between the origin and $t = -1$ the contour can be extended to include the point $t = -1$; hence

$$\int_{\infty e^{i\theta}}^{(0+)} = \int_{\infty e^{i\theta}}^{-1} + \int_{-1}^{\infty e^{i(\theta + 2\pi)}} . \tag{4.20}$$

Using (4.20) and (4.17)-(4.19) yields

$$\tilde{b}_j - b_j = (2\beta_2)^{\alpha-1} \frac{2\pi i e^{i\pi a}}{\Gamma(1 - a)} e^{-\xi/2} U(a,\alpha;\xi) . \tag{4.21}$$

Using (2.23) together with (2.17) one finds that

$$B_j = [e^{i2\pi a} - 1]^{-1} \left\{ (\tilde{B}_j - B_j) - B_o \right\} , \tag{4.22}$$

which, for $\varepsilon^2 = 0$, becomes

$$b_j = [e^{i2\pi a} - 1]^{-1} \left\{ (\tilde{b}_j - b_j) - b_o \right\} \quad . \tag{4.23}$$

Using (4.21) to replace the combination $\tilde{b}_j - b_j$ in (4.23) and employing the identity $\Gamma(a)\Gamma(1-a) = \pi/\sin(a\pi)$ gives

$$b_j = (2\beta_2)^{\alpha-1}\Gamma(a)e^{-\xi/2}\, U(a,\alpha;\xi) - \frac{e^{-i\pi a}\, b_o}{2i\, \sin(\pi a)} \quad . \tag{4.24}$$

The relation (2.23) for $\varepsilon^2 = 0$ gives

$$\tilde{b}_j = b_j(0,1) + b_o = e^{i2\pi a}\, b_j + b_o \quad . \tag{4.25}$$

Using (4.25) to replace b_j by $\tilde{b}_j$ in (4.24) gives

$$\tilde{b}_j = (2\beta_2)^{\alpha-1}\, e^{i2\pi a}\Gamma(a)e^{-\xi/2}\, U(a,\alpha;\xi) - \frac{e^{-i\pi a}\, b_o}{2i\, \sin(\pi a)} \quad . \tag{4.26}$$

With (4.11) the relations (4.24) and (4.26) can be used to express b_j and $\tilde{b}_j$ entirely in terms of the Kummer functions U and M,

$$b_j(\xi) = (2\beta_2)^{\alpha-1}\, e^{-\xi/2}\{\Gamma(a)U(a,\alpha;\xi) - \frac{\pi\, \exp(-i\pi a)\Gamma(\alpha-a)}{\sin(\pi a)\Gamma(\alpha)\Gamma(1-a)}\, M(a,\alpha,\xi)\} \tag{4.27}$$

and

$$\tilde{b}_j(\xi) = (2\beta_2)^{\alpha-1}\, e^{-\xi/2}\{\Gamma(a)\exp(2\pi i a)U(a,\alpha;\xi) - \frac{\pi\, \exp(-i\pi a)\Gamma(\alpha-a)}{\sin(\pi a)\Gamma(\alpha)\Gamma(1-a)}\, M(a,\alpha;\xi)\}, \tag{4.28}$$

where again $a = \alpha/2 - \beta_o$ and $\xi = 2\beta_2 z$.

Expressions for B_j and $\tilde{B}_j$ valid to order ε^2 can be obtained by using (4.27) and (4.28) in the expansion (4.1) in the same fashion that the expression (4.12) for B_0 is obtained from (4.1) using $u_0 = b_0$. We do not write out the corresponding expressions for B_j and $\tilde{B}_j$ here but only note that the functions b_j and $\tilde{b}_j$ deduced from (4.2) are obtained under the restriction $|z| > |z_0| > 0$ and within the argument range (4.15). In other words, B_j and $\tilde{B}_j$ can not be evaluated at the point $z = 0$ using the expansion in ε^2 technique. The problem of applying (4.1) at the origin for the solutions B_j and $\tilde{B}_j$ arises because the function $U(a,\alpha;\zeta)$ in the expressions for b_j and $\tilde{b}_j$ is singular at the origin ($z = 0$) for $\alpha \geq 1$. However, the behavior of the solutions B_j and $\tilde{B}_j$ for $|z| \to 0$ for all values of α can be found by employing the relations (2.18)-(2.23). For example, multiplying (2.22) by $e^{i2\pi\alpha}$- and using (2.9), (2.10) and (2.17) yields

$$A_2(0,1) = -B_1(0,1) + e^{i2\pi\alpha}\,\tilde{B}_3 \ . \tag{4.29}$$

Using (2.23) with $j = 1$ in (4.29) and (2.19) and (2.22) in the resulting expression gives

$$\tilde{B}_3 = [e^{i2\pi\alpha} - 1]^{-1}\,\{A_2(0,1) + A_1 + A_3(0,1) - B_0\} \ . \tag{4.30}$$

The expression (4.12) can be used to evaluate B_0, for all $|z| < \infty$, while the power series expansion (3.24) can be used to evaluate the functions A_j for small argument ($|z| << 1$). Thus, expressions such as (4.30) are particularly useful in evaluating B_j and $\tilde{B}_j$ in the neighborhood of the origin. For large values of $|z|$,

on the other hand, B_j and $\tilde{B}_j$ are more conveniently expressed using the ϵ^2 expansion of (4.1) in terms of b_j and $\tilde{b}_j$, respectively.

Since the solutions related to the Kummer function $U(a,\alpha;\xi)$ contain the combination $\tilde{b}_j - b_j$ [c.f. (4.21)] it is useful to construct the combination $\tilde{B}_3 - B_3$ in a form that can be evaluated as $|z| \to 0$. To do this we multiply (2.23) by $e^{-i2\pi\alpha_-}$ and use (2.17) to obtain

$$B_3 = \tilde{B}_3(0,-1) - B_0(0,-1) \ . \tag{4.31}$$

Multiplying (4.30) by $e^{-i2\pi\alpha_-}$ and using (4.31) in the resulting relation gives

$$B_3 = [e^{i2\pi\alpha} - 1]^{-1} \{A_2 + A_1(0,-1) + A_3 - B_0(1,0)\} \ . \tag{4.32}$$

Finally, combining (4.30) and (4.32) yields the desired combination

$$\tilde{B}_3 - B_3 = [e^{i2\pi\alpha} - 1]^{-1} \{(e^{i2\pi\alpha_-} - 1)[A_2 + A_1(0,-1) + A_3] - (1 - e^{i2\pi\alpha_+})B_0\} \tag{4.33}$$

Expressions similar to (4.33) involving B_2 and B_1 rather than B_3 can be found by using (2.18)-(2.22). The expression (4.33) can be evaluated at integer values of α by assuming that $\tilde{B}_3 - B_3$ is an entire function of α and then using L'Hospital's rule to obtain

$$\begin{aligned} \tilde{B}_3 - B_3 = \Big\{ & [A_2(0,1) + A_3(0,1) + A_1 + B_0(1,0)]/2 \\ & + (1/2\pi i)(e^{i2\pi\alpha_-} - 1)[\partial_\alpha A_2 + \partial_\alpha A_1(0,-1) + \partial_\alpha A_3] \\ & + (1/2\pi i)(e^{i2\pi\alpha_+} - 1)\partial_\alpha B_0\Big] \Big|_{\alpha=n} \ . \end{aligned} \tag{4.34}$$

where $n = 0,\pm1,\pm2,\ldots$. The expressions (4.33) and (4.34) show that the combination $\tilde{B}_3 - B_3$ is finite and non-singular at the origin for all values of α. On the other hand, the expression (4.21) with $j = 3$ indicates that $\tilde{b}_3 - b_3$ is singular at the origin for $\alpha \geq 1$. Thus the exact solutions of (1.3) are rigorously well behaved at the origin although the restricted expressions obtained by using an expansion in ε^2 indicate otherwise, which is a consequence of the singular perturbation character of this problem. Expressions for $\tilde{B}_2 - B_2$ and $\tilde{B}_1 - B_1$ are readily obtained from (4.33) using (2.18)-(2.23).

Finally, it is instructive to consider a special case in which the parameters α and β have the values

$$\alpha = \nu \; ; \qquad \beta = \nu/2 + \mu \; , \tag{4.35}$$

where ν is a positive integer and $\mu = 0,1,2,\ldots$. In this case

$$\alpha_+ = \nu - 1 + \mu \; ; \tag{4.36}$$

and

$$\alpha_- = -(\mu + 1) \; . \tag{4.37}$$

In the integral representation (2.7) there is now only an isolated pole of order $\mu + 1$ at the point $s = \beta_2$. The points $s = \pm\beta_2$ are no longer branch points and the s-plane is no longer cut by branch lines, so that $B_j(0,1) = B_j$ and (2.23) then gives

$$\tilde{B}_j - B_j = B_o \; . \tag{4.38}$$

The contour B_o now encloses the pole at $s = \beta_2$ and from Cauchy's Theorem we immediately have

$$B_o = 2\pi i R(\beta_2) \ , \tag{4.39}$$

where $R(\beta_2)$ is the residue of the pole at $s = \beta_2$. Using (4.36) and (4.37) one obtains from the integrand of (2.7) the expression

$$R(\beta_2) = \frac{1}{\mu!} \frac{d^\mu}{ds^\mu} \left[(s + \beta_2)^{\nu-1+\mu} \ e^{-\varepsilon^2 s^3/3} \ e^{-s\tilde{z}} \right] \Big|_{s=\beta_2} \ . \tag{4.40}$$

Making use of Leibniz's Theorem the expression (4.40) can also be written as

$$R(\beta_2) = \frac{1}{\mu!} \sum_{j=0}^{\mu} \binom{\mu}{j} \ E_j \ \frac{d^{\mu-j}}{ds^{\mu-j}} \left[(s + \beta_2)^{\nu-1+\mu} \ e^{-s\tilde{z}} \right] \Big|_{s=\beta_2} \ , \tag{4.41}$$

where $\binom{\mu}{j}$ is the usual Binomial coefficient and

$$E_j = \frac{d^j}{ds^j} \left(e^{-\varepsilon^2 s^3/3} \right) \Big|_{s=\beta_2} \ . \tag{4.42}$$

By defining the small quantity $\sigma_o \equiv \varepsilon^{2/3}\beta_2$ and letting $x = (s + \beta_2)\tilde{z}$, (4.41) becomes

$$R(\beta_2) = \frac{e^{-\sigma_o{}^3/3}}{\mu!} \ e^{\beta_2 \tilde{z}} \sum_{j=0}^{\mu} \binom{\mu}{j} \ [\sigma_o/\beta_2]^j \ z^{1-\nu-j} \ T_j$$

$$\times \frac{d^{\mu-j}}{dx^{\mu-j}} \left[x^{\nu-1+\mu} \ e^{-x} \right] \Big|_{s=2\beta_2\tilde{z}} \ , \tag{4.43}$$

where the polynomials T_j are given by

$$T_j = e^{\sigma_o{}^3/3} \frac{d^j}{dt^j} (e^{-t^3/3}) \Big|_{t=\sigma_o} \tag{4.44}$$

and $T_o = 1$. The expression (4.43) can be further simplified by using Rodrigues' Formula[13] for the Laguerre Polynomials

$$L_{\mu-j}^{\nu-1+j} (x) = \frac{1}{(\mu-j)!} e^x x^{1-\nu+j} \frac{d^{\mu-j}}{dx^{\mu-j}} (x^{\nu-1+\mu} e^{-x}) . \tag{4.45}$$

Using (4.45) in (4.43) one obtains from (4.39)

$$\tilde{B}_j - B_j = B_o = 2\pi i (2\beta_2)^{\nu-1} e^{-\beta_2 \tilde{z}} e^{-\sigma_o{}^3/3}$$

$$\times \left\{ \sum_{j=0}^{\mu} \frac{(2\sigma_o)^j}{(j)!} T_j L_{\mu-j}^{\nu-1+j} (2\beta_2 \tilde{z}) \right\} \tag{4.46}$$

for $\mu = 0,1,2,\ldots$, and where $\tilde{z} = z + \sigma_o{}^3/\beta_2$. Using (4.44) to evaluate terms in (4.46) results in

$$B_o = 2\pi i (2\beta_2)^{\nu-1} e^{-\beta_2 z} L_\mu^{\nu-1} (2\beta_2 z) + O(\sigma_o{}^3) . \tag{4.47}$$

Note that $\sigma_o{}^3 = \varepsilon^2 \beta_2{}^3$, so that the correction terms to B_o as given by (4.47) are of order ε^2.

5. Application to Physical Problems

In applying the solutions of (1.3) to a physical problem one needs to evaluate the solutions A_j, B_o, B_j and $\tilde{B}_j$ in the vicinity of the real axis (Im $z \to 0+$). However, the expressions given in Secs. 3 and 4 for some of the solutions are valid only in certain sectors of the complex z-plane. Since some of these sectors contain only a portion of the real axis, the expressions given must be extended by means of analytic continuation to include the entire region of physical interest. The process of analytic continuation leads to a mixing of the solutions of the thermal and cold plasma classes. This mixing embodies the physical phenomenon of mode conversion.

In constructing analytic continuations of solutions we will take the imaginary part of the independent variable z to be small and positive. This assumption leads to exponential decay of waves in the direction of propagation and is justified on physical grounds because it corresponds to adiabatic switch-on of the exciter at frequency ω. The analytic continuation of the solutions of (1.3) can be accomplished by using the relations (2.18)-(2.23) which are derived by applying Cauchy's Theorem to the contours defining the various solutions.

The asymptotic expressions for the solutions A_j as given by (3.7) are valid in sectors of aperture $4\pi/3$ as given by (3.4). Since the solution A_1 is defined in the sector $5\pi/3 < \theta < 3\pi$ ($z = |z|e^{i\theta}$), which includes the entire region of physical interest, it needs no analytic continuation. Just above the negative real axis $\theta = 3\pi - \Delta$, where Δ is a positive infinitesimal, the term $\exp(-i\zeta)$ in the asymptotic expression (3.7) for A_1 varies as $\exp|\zeta|$. Thus A_1 is exponentially growing near the negative real axis. Along the positive real axis where $\theta = 2\pi + \Delta$ the term $\exp(-i\zeta)$ varies as $\exp i|\zeta|$ so that A_1 represents an outward propagating

wave in the WKB sense. The solution A_2 is defined in the region $\pi/3 < \theta < 5\pi/3$ which includes the region of physical interest only near the negative real axis where $\theta = \pi - \Delta$. The term $\exp(-i\zeta)$ in (3.4) for j=2 then varies as $\exp(-|\zeta|)$ so that A_2 is exponentially decaying for $\mathrm{Re}(z) < 0$. To analytically continue A_2 we use the relations (2.18), (2.20) and (2.22) to obtain (see Fig. 4)

$$A_2 = -A_3 - B_2 + \tilde{B}_2(1,0) - A_1(1,0), \tag{5.1}$$

for $\mathrm{Re}(z) > 0$. All of the functions on the right-hand side of (5.1) are defined in sectors that include the region just above the positive real axis as can be verified by (3.4) and (4.15). The relation (5.1) indicates that the solution A_2 undergoes mode conversion when the $\mathrm{Re}(z)$ changes sign. In this paper we use the term mode conversion to denote a process wherein a solution of one class produces a solution of the other class. For example, as indicated by (5.1), a solution of the thermal class, A_2, near the negative real axis, leads to solutions of the cold mode class as well as thermal mode class solutions near the positive real axis. Finally, the domain in which the solution A_3 is defined includes the region above the positive real axis but not the region above the negative real axis. Near the positive real axis $\theta = \Delta$ for j=3 and A_3 varies as $e^{-i|\zeta|}$ thus representing, in the WKB sense, an inward propagating wave. Using (2.18), (2.21) and (2.20) to analytically continue A_3 we find that (see Fig. 4)

$$A_3 = -A_1(0,-1) - B_3 + \tilde{B}_3(1,0) - A_2 \ , \tag{5.2}$$

where all of the functions on the right-hand side of (5.2) are defined in the region just above the negative real axis.

The expressions derived for the solutions B_j and $\tilde{B}_j$ are also valid only in certain sectors of the z-plane as indicated by (4.15). The solutions B_3 and $\tilde{B}_3$ are defined for the entire region above the real axis and need no analytic continuation. The solutions B_2 and $\tilde{B}_2$ are defined only in the region above the positive real axis and must be continued by using (2.21) and (2.22) from which we obtain

$$B_2 = B_3 + A_1(0,-1) \tag{5.3a}$$

and

$$\tilde{B}_2 = \tilde{B}_3 + A_1 \tag{5.3b}$$

Both functions on the right-hand side of (5.3a) and (5.3b) are defined in the region just above the negative real axis. B_2 and $\tilde{B}_2$ both undergo mode conversion when Re(z) changes sign as indicated by (5.3a) and (5.3b) because they generate a solution of the thermal mode class in addition to a solution of the cold mode class. The solutions B_1 and $\tilde{B}_1$ are defined for the region just above the negative real axis and can be continued to include the region just above the positive real axis by using (2.18) and (2.19) to obtain

$$B_1 = B_2 + A_3 \ , \tag{5.4a}$$

and

$$\tilde{B}_1 = \tilde{B}_2 + A_3(0,1) \ . \tag{5.4b}$$

Again the solutions B_1 and $\tilde{B}_1$ undergo mode conversion when Re(z) changes sign.

In addition to having expressions for the solutions in the region above the real axis a useful set of four linearly independent solutions must be selected from the general set in order to solve a well posed problem of physical interest. In particular, we have in mind applying the solutions of (1.3) to the inhomogeneous problem in which a driving source is present in the plasma. We thus shall discuss four linearly independent solutions that are convenient in constructing a Green's function for (1.3). The linear independence of a solution set can be formally established by evaluating the system Wronskian. Rather than perform this calculation we defer it to a later paper and only present here a heuristic argument for linear independence.

A Green's function must satisfy certain boundary conditions and we impose these beforehand in choosing our solution set. The boundary conditions we impose are: 1) wave-like solutions must correspond to transport of energy away from the source, and 2) solutions must be bounded as $|\mathrm{Re}(z)| \to \infty$. Since the thermal mode and cold plasma mode classes of solutions have vastly different scale sizes away from plasma resonance, our strategy for identifying a linearly independent set is to select one pair of linearly independent solutions from each class. We are then assured of the linear independence of pairs of solutions from different classes because of their different scale sizes. From the cold mode class of solutions we choose the pair B_2, $\tilde{B}_2$ while from the thermal class of solutions we choose the pair A_1, A_2.

From the solution pair B_2, $\tilde{B}_2$ we next construct a pair of linearly independent solutions, one of which is bounded as $z \to \infty$, while the other is bounded for $z \to -\infty$. This solution pair is

$$B_R = [(2\beta_2)^{1-\alpha}/2\pi i]\,\Gamma(-\alpha_-)\, e^{-i\pi\alpha_-}\{\tilde{B}_2(\alpha,\beta_1,\beta_2,\varepsilon^2,\xi) - B_2(\alpha,\beta_1,\beta_2,\varepsilon^2,\xi)\}\,, \tag{5.5}$$

$$B_L = [(2\beta_2)^{1-\alpha}/2\pi i]\Gamma(-\alpha_+)\, e^{-i\pi\alpha_+}\{\tilde{B}_2(\alpha,-\beta_1,\beta_2,-\varepsilon^2,-\xi) - B_2(\alpha,-\beta_1,\beta_2,-\varepsilon^2,-\xi)\}. \tag{5.6}$$

Note that in (5.6) we have used the transformation (2.12) so that we are assured B_L is a solution to (1.3). The normalization coefficients in (5.5) and (5.6) have been determined using (4.27) and (4.28) and are chosen so that the expressions reduce, when $\varepsilon^2 = 0$, to the simple forms given below,

$$B_R = e^{-\xi/2}\, U(a,\alpha;\xi), \tag{5.7}$$

$$B_L = e^{+\xi/2}\, U(\alpha - a,\alpha;-\xi)\,, \tag{5.8}$$

where $a = \alpha/2 - \beta_2$. In the notation of Slater[14] these two solutions are then

$$B_R = e^{-\xi/2}\, y_5\,, \tag{5.9}$$

$$B_L = e^{-\xi/2}\, y_7\,. \tag{5.10}$$

so that using (5.9) and (5.10) together with (4.1) we find that the Wronskian of B_R and B_L is

$$W(B_R,B_L) = e^{i\pi(\alpha/2+\beta_o)}(\xi)^{-\alpha} + O(\epsilon^2) \ , \tag{5.11}$$

where $\xi = 2\beta_2 z$. In (5.11) we have again assumed that Im(z) is positive and have ignored contributions to the Wronskian arising from mode conversion. Mode conversion contributes terms to the Wronskian that are a product of cold and thermal terms and thus are rapidly oscillating. The function B_R is bounded as z approaches positive real infinity while B_L is bounded as z approaches negative real infinity.

The asymptotic form of the two thermal modes A_1 and A_2 has been discussed before. The function A_2 is exponentially decaying along the negative real axis while A_1 is exponentially growing. Thus A_2 and A_1 are clearly linearly independent. Near the positive real axis A_1 represents an outward propagating wave while from (5.1) we see that A_2, while undergoing mode conversion, contains an A_3 term which represents an inward propagating wave so that A_1 and A_2 are again linearly independent.

The solution set B_R, B_L, A_2, A_1 is convenient for constructing a Green's function. If we denote the source location by z' then the solution pair B_L, A_2 can be used exclusively for $Re(z-z') < 0$ because they are the only pair bounded at negative real infinity, while the remaining pair B_R, A_1 can be used exclusively for $Re(z-z') > 0$ because they are the only pair bounded at positive real infinity. While we do not construct a Green's function here we can use the solution set B_R, A_1, B_L, A_2 to illustrate the type of mode conversion that may occur in a plasma with a driving source.

As an illustration of mode conversion in a physical problem, consider the solution B_R for $Re(z) > 0$. This cold mode solution as given by (5.5) depends upon B_2 and $\tilde{B}_2$ which can be analytically continued to the region just above the negative real axis by using (5.3a) and (5.3b) from which we obtain, for $Re(z) < 0$,

$$B_R = [(2\beta_2)^{1-\alpha}/2\pi i]\Gamma(-\alpha_-)e^{-i\pi\alpha_-}\{\tilde{B}_3(\alpha,\beta_1,\beta_2,\varepsilon^2,\xi) - B_3(\alpha,\beta_1,\beta_2,\varepsilon^2,\xi)\}$$

$$- [(2\beta_2)^{1-\alpha}/\Gamma(1+\alpha_-)]e^{-i2\pi\alpha_-} A_1(\alpha,\beta_1,\beta_2,\varepsilon^2,\xi) \ . \qquad (5.12)$$

We have already indicated that A_1 is exponentially decaying near the negative real axis while the combination, $\tilde{B}_3 - B_3$, is defined in the region above the negative real axis and according to (4.21) is proportional to the hypergeometric function $U(a,\alpha;\xi)$ for $\varepsilon^2 = 0$. The expression (5.12) illustrates mode conversion in that a solution of the cold class on one side of plasma resonance consists of a combination of cold and thermal modes on the other side of resonance.

We note that in this particular example the amount of mode converted thermal mode is proportional to $1/\Gamma(1+\alpha_-)$, and thus can be zero when

$$1 + \alpha_- = \alpha/2 - \beta = -\ell \ , \qquad (5.13)$$

where $\ell = 0,1,2,\ldots$. When α is an integer, as is the case for a plasma, the condition (5.13) is identical to (4.35). In Section 4 we found that under these conditions the cold mode solutions were everywhere proportional to B_{ℓ} which in turn could be expressed as a sum involving Laguerre Polynomials [see (3.46)]. Thus at certain special values of the parameter β the phenomenon of mode conversion does not occur in the sense that the amplitude of the thermal mode is zero and furthermore, at these values of β the cold solutions are proportional to Laguerre Polynomials for $\varepsilon^2 = 0$.

The quenching of the mode conversion process does not occur for all possible solutions, e.g., the solutions B_L for $Re(z) < 0$, corresponding to a source located in the region $z > 0$. Using (5.6) and the relations (5.3a) and (5.3b) with the proper parameter values, we obtain the analytic continuation, for $Re(z) > 0$,

$$B_L = [(2\beta_2)^{1-\alpha}/2\pi i]\Gamma(2+\alpha_+)\, e^{-i\pi\alpha_+} \{\tilde{B}_3(\alpha,-\beta_1,\beta_2,-\varepsilon^2,-\xi) - B_3(\alpha,-\beta_1,\beta_2,-\varepsilon^2,-\xi)\}$$

$$- [(2\beta_2)^{1-\alpha}/\Gamma(1+\alpha_+)]\; e^{-i2\pi\alpha_+} A_1(\alpha,-\beta_1,\beta_2,-\varepsilon^2,-\xi)\ . \qquad (5.14)$$

Since α and β are positive, $1/\Gamma(1+\alpha_+) = 1/\Gamma(\alpha/2+\beta)$ is never zero and mode conversion always occurs in this case. Furthermore, the mode conversion process is not restricted to the generation of thermal modes by cold modes. The thermal modes also undergo the mode conversion process and generate cold modes. Although the solution A_1 does not undergo mode conversion when $Re(z)$ changes sign, the solution A_2 does as is illustrated by the analytic continuation of A_2 given in (5.1).

6. Conclusions:

By applying the Laplace integral technique we have obtained integral representations of the solutions of the fourth order differential equation (1.3). The solutions are distinguished by the contours along which the integral is evaluated. The solutions A_j are obtained by integrating along contours having both end-points at infinity and have been identified as belonging to a class of solutions characterized by short scale lengths and thus are referred to as thermal modes. The solutions B_0, B_j and $\tilde{B}_j$ are obtained by integrating along contours with at least one end-point at the branch point $s = -p_2$ and belong to a class of solutions characterized by long scale lengths and are referred to as cold modes. The properties of the exact solutions A_j, B_0, B_j and $\tilde{B}_j$ have been elucidated by expressing them in terms of more familiar functions using power series and asymptotic expansions.

The solutions A_j have been evaluated for large and small values of the independent variable z by using different techniques. A power series expansion in z has been derived in (3.24) in order to determine the solutions A_j in the neighborhood of the origin. The solutions A_j are clearly finite and well behaved in the vicinity of the origin. For large values of z the functional form of the solutions A_j has been determined in (3.11) using the saddle point method of integration to obtain the leading term in an asymptotic expansion. For real values of the independent variable these asymptotic expressions represent either exponentially decaying or growing solutions or propagating wave-like solutions.

Expressions for the solutions B_0, B_j, and $\tilde{B}_j$ have been obtained by expanding the integral representation in powers of ϵ^2. This technique allows an expression to be obtained for the exact solutions B_0, B_j, $\tilde{B}_j$ in terms of the corresponding solutions b_0, b_j, $\tilde{b}_j$ of the second order differential equation obtained from (1.3) by setting $\epsilon^2 = 0$. The expansion (4.12) obtained in this manner for the

solution B_0 involves the Kummer function $M(b,c;z)$ and is valid in the entire z-plane ($|z| < \infty$). In particular the solution B_0 can be evaluated in the neighborhood of the origin using (4.12) and thus is useful in evaluating other members of the cold mode solution class near the origin.

An expansion in powers of ϵ^2 can be obtained for the solutions B_j and $\tilde{B}_j$ but involves the restriction $|z| > |z_0| > 0$. The expansion involves the corresponding solutions b_j and $\tilde{b}_j$ which contain the Kummer function $U(b,c;z)$ which is not bounded at the origin for $Re(c) \geq 1$. The ϵ^2 expansion is helpful in evaluating the solutions B_j and $\tilde{B}_j$ for large values of z. The solutions B_j and $\tilde{B}_j$ can be evaluated in the neighborhood of the origin by using Cauchy's theorem to establish relationships among the various solutions as given in (2.18)-(2.23). Thus the solutions B_j and $\tilde{B}_j$ can be expressed entirely in terms of various combinations of the solutions A_j and B_0 as shown for $\tilde{B}_3$ in (4.30). Since expressions for the solutions A_j and B_0 valid in the neighborhood of the origin have been obtained the solutions B_j and $\tilde{B}_j$ can also be, in principle, evaluated there. Unlike the associated solutions to the second order differential equation, b_j and $\tilde{b}_j$, which can have divergent behavior at the origin for $\alpha \geq 1$, the solutions B_j and $\tilde{B}_j$ are always finite at the origin. The physical interpretation of this result is that the inclusion of thermal effects keeps the amplitude of the electric field finite at plasma resonance through the production of short scale thermal modes. The production of short scale waves near plasma resonance involves the process of mode conversion.

For certain values of the parameters, α and β, namely α a positive integer and $\beta = \epsilon^2\beta_2^3/2 + \beta_1/2\beta_2$ a positive half-integer, the topology of the integration plane is greatly simplified. While the sector structure in the integration

plane remains, there are no branch points but only an isolated pole. The quantities α_+ and α_- have integer values under these conditions so that the phase factors $\exp(i2\pi m\alpha_+)$ and $\exp(i2\pi n\alpha_-)$ are unity and as indicated by (2.17) all solutions X(m,n) are equivalent to the solution X evaluated on the principal sheet. The combination of solutions $\tilde{B}_j - B_j$ is equivalent to the solution B_o as indicated in (4.38). Furthermore, the solution B_o can be expressed as a series of generalized Laguerre Polynomials as given in (4.46) which is convenient for numerically evaluating quantities for physical applications. Finally, we note that as shown in (4.34) the combination $\tilde{B}_3 - B_3$ generally contains an admixture of the thermal mode solutions A_j. For these special parameter values, however, the combination $\tilde{B}_3 - B_3 = B_o$, hence it contains no thermal mode solutions. Physically this indicates that mode conversion does not occur at these special parameter values.[15]

The asymptotic expressions given for the solutions A_j, B_j and $\tilde{B}_j$ are defined in certain sectors of the z-plane as given by (3.4) and (4.15). Not all of these sectors contain the region just above the real axis which is the region of interest in physical applications. The solutions can be analytically continued, however, and it is this process which gives rise to the phenomenon of mode conversion. A solution of either the thermal or cold mode class on one side of plasma resonance gives rise to a combination of both classes on the other side of resonance. Physically the mode conversion process serves to limit the amplitude of the solutions at plasma resonance. Specifically, the solutions of the purely cold plasma ($\varepsilon^2 = 0$) which exhibit singularities at the origin now correspond to solutions which are finite at the origin but produce thermal modes through the mode conversion process which carry wave energy away form the resonance region. In addition, for special values of the

parameters, it is possible to construct cold mode class solutions which are finite at the origin without generating thermal mode class solutions. This quenching of the mode conversion process corresponds to a change in the topology of the integration plane in which the branch points become an isolated pole.

ACKNOWLEDGEMENTS

We are grateful to Professor Earl A. Coddington for illuminating discussions concerning integral representations. This work has been supported by the Office of Naval Research under contract number ONR N000014-80-C-0373.

REFERENCES

1. J.E. Maggs and G.J. Morales, "Electrostatic Modes in a Magnetized Plasma With a Longitudinal Density Gradient", J. of Plasma Phys., (in press, 1983).
2. W. Wasow, "Asymptotic Solution of the Differential Equation Governing Hydrodynamic Stability in a Domain Containing a Transition Point", Annals of Mathematics, 58, 222 (1953).
3. A.L. Rabenstein, "Asymptotic Solutions of $u^{iv} + \lambda^2(zu'' + \alpha u' + \beta u) = 0$ for Large $|\lambda|$", Archives for Rational Mechanics and Analysis 1, 418 (1958).
4. E.A. Coddington and N. Levinson, Theory of Ordinary Differential Equations (McGraw-Hill Book Co., Inc., New York, 1955), Section 5.8.
5. Alfredo Baños, Jr., Dipole Radiation in the Presence of a Conducting Half-Space (Pergamon Press, New York, 1966), Chapter 3.
6. E.T. Whittaker and G.N. Watson, A Course of Modern Analysis (Cambridge University Press, 1963), Section 2.53.
7. Ibid., Sections 3.33 and 3.7.
8. See footnote 3.
9. A. Erdélyi, W. Magnus, F. Oberhettinger, and F. Tricomi, Higher Trancendental Functions [Bateman Manuscript Project (McGraw-Hill, New York, 1953)], Vol. 1, Equation 1.6.6.
10. L.J. Slater, "Confluent Hypergeometric Functions", in Handbook of Mathematical Functions with Formulas, Graphs and Mathematical Tables, edited by M. Abramowitz and I.A. Stegun (U.S. Government Printing Office, Washington, D.C., 1964).
11. A. Erdélyi, W. Magnus, F. Oberhettinger and F. Tricomi, op. cit., Section 6.11.1.

12. Ibid., Section 6.11.2.

13. V.W. Hochstrasser, "Orthogonal Polynomials", in Handbook of Mathematical Functions with Formulas, Graphs and Mathematical Tables, edited by M. Abramowitz and I.A. Stegun (U.S. Government Printing Office, Washington, D.C., 1964).

14. See footnote 10.

15. G.J. Morales and J.E. Maggs, "Guided Modes Between Upper Hybrid and Plasma Resonance", J. of Plasma Phys., (in press, 1983).

APPENDIX

A.1 General expression for the derivatives of u(z)

The nth derivative of the function $u(\alpha,\beta_1,\beta_2,\varepsilon^2,z)$ with respect to z, which we denote as $u^{(n)}$, can be obtained from the integral representation (2.7).

$$u^{(n)}(\alpha,\beta_1,\beta_2,\varepsilon^2,z) = (-)^n \int_C s^n(s-\beta_2)^{\alpha-}(s+\beta_2)^{\alpha+} \exp(-s^3\varepsilon^2/3-s\tilde{z})ds \ , \qquad (A.1.1)$$

where C is any of the contours discussed in Section 2. To find an expression for the first derivative we note that

$$s = (1/4\beta_2)[(s+\beta_2)^2 - (s-\beta_2)^2], \qquad (A.1.2)$$

together with

$$u(\alpha+2,\beta_1+2\beta_2,\beta_2,\varepsilon^2,z) = \int_C (s+\beta_2)^2(s+\beta_2)^{\alpha+}(s-\beta_2)^{\alpha-} \exp(-s^3\varepsilon^2/3-\tilde{z}s)ds \ ; \qquad (A.1.3)$$

and

$$u(\alpha+2,\beta_1-2\beta_2,\beta_2,\varepsilon^2,z) = \int_C (s-\beta_2)^2(s+\beta_2)^{\alpha+}(s-\beta_2)^{\alpha-} \exp(-s^3\varepsilon^2/3-\tilde{z}s)ds \ . \qquad (A.1.4)$$

Using (A.1.1) with n = 1, the expression (A.1.2) together with (A.1.3) and (A.1.4) gives

$$u^{(1)}(\alpha,\beta_1,\beta_2,\varepsilon^2,z) = (-1/4\beta_2)[u(\alpha+2,\beta_1+2\beta_2,\beta_2,\varepsilon^2,z) - u(\alpha+2,\beta_1-2\beta_2,\beta_2,\varepsilon^2,z)] \ . \qquad (A.1.5)$$

The second derivative of u can be found in a similar fashion by using the expression

$$s^2 = (s - \beta_2)(s + \beta_2) + \beta_2{}^2 \ ; \tag{A.1.6}$$

we then obtain

$$u^{(2)}(\alpha,\beta_1,\beta_2,\varepsilon^2,z) = u(\alpha+2,\beta_1,\beta_2,\varepsilon^2,z) + \beta_2{}^2\, u(\alpha,\beta_1,\beta_2,\varepsilon^2,z) \ . \tag{A.1.7}$$

Repeated use of the expression (A.1.7) yields

$$u^{(n)}(\alpha,\beta_1,\beta_2,\varepsilon^2,z) = \sum_{j=0}^{n} \left\langle \begin{matrix} n \\ j \end{matrix} \right\rangle \ \beta_2{}^{2(n-j)} u(\alpha+2j,\beta_1,\beta_2,\varepsilon^2,z) \ , \tag{A.1.8}$$

where $n = 0,1,2,3,\ldots$ and $\left\langle \begin{matrix} n \\ j \end{matrix} \right\rangle = n!/(n-j)!j!$, are the binomial coefficients. Application of (A.1.5) to (A.1.8) then yields

$$u^{(2n+1)}(\alpha,\beta_1,\beta_2,\varepsilon^2,z) = (1/4) \sum_{j=0}^{n} \left\langle \begin{matrix} n \\ j \end{matrix} \right\rangle \ \beta_2{}^{2(n-j)-1}$$

$$\times \left[u(\alpha+2(j+1),\beta_1-2\beta_2,\beta_2,\varepsilon^2,z) - u(\alpha+2(j+1),\beta_1+2\beta_2,\beta_2,\varepsilon^2,z)\right] \ . \tag{A.1.9}$$

A.2 A series expansion of u in powers of ε^2

In this appendix we outline the procedure for obtaining a series expansion of $u(\alpha,\beta_1,\beta_2,\varepsilon^2,z)$ in powers of ε^2 and explicitly calculate the first two coefficients of this series. We first assume that the integrand of (2.7) is an analytic function of ε^2 in the vicinity of $\varepsilon^2 = 0$ and expand a portion of the

integrand in a Taylor's series about the point $\varepsilon^2 = 0$. We will discuss the validity of this assumption later. The integrand of (2.7) depends on ε^2 indirectly through the parameters α_+,α_- and directly as $\exp[-\varepsilon^2(s^3/3 + \beta_2{}^2 s)]$. Thus part of the integrand in (2.7) can be written as

$$(s + \beta_2)^{\alpha_+}(s - \beta_2)^{\alpha_-} \exp[-\varepsilon^2(s^3/3 + \beta_2{}^2 s)] \tag{A.2.1}$$

$$\simeq (s + \beta_2)^{a_+}(s - \beta_2)^{a_-} \left\{1 - \varepsilon^2\{s^3/3 + \beta_2{}^2 s - (\beta_2{}^3/2)\ell n[(s+\beta_2)/(s-\beta_2)]\}; \quad +.....\right.$$

where we have explicitly shown only the first two terms of the Taylor series expansion. The parameters a_+ and a_- are simply the values of α_+ and α_- at $\varepsilon^2 = 0$, namely,

$$a_+ = \alpha_+(\varepsilon^2 = 0) = \alpha/2 - 1 + \beta_1/2\beta_2 \; ; \tag{A.2.2}$$

$$a_- = \alpha_-(\varepsilon^2 = 0) = \alpha/2 - 1 - \beta_1/2\beta_2 \; . \tag{A.2.3}$$

Using (A.2.1) in (2.7) we obtain

$$u(\alpha,\beta_1,\beta_2,\varepsilon^2,z) = \int_C (s - \beta_2)^{a_-}(s + \beta_2)^{a_+} e^{-zs}\, ds$$

$$- \varepsilon^2\{\beta_2{}^2 \int_C s(s - \beta_2)^{a_-}(s + \beta_2)^{a_+} e^{-zs} ds + (1/3)\int_C s^3(s - \beta_2)^{a_-}(s + \beta_2)^{a_+} e^{-zs} ds$$

$$-(\beta_2{}^3/2)\int_C \ell n[(s+\beta_2)/(s-\beta_2)](s + \beta_2)^{a_+}(s - \beta_2)^{a_-} e^{-zs} ds\} + ... \tag{A.2.4}$$

Noting that

$$\int_C \ln[(s + \beta_2)/(s - \beta_2)](s + \beta_2)^{a_+}(s - \beta_2)^{a_-} e^{-zs}\, ds$$

$$= 2\beta_2 \frac{\partial}{\partial \beta_1} \int_C (s + \beta_2)^{a_+}(s - \beta_2)^{a_-} e^{-zs}\, ds\ , \qquad (A.2.5)$$

and using (A.1.1) together with (A.1.9) we obtain

$$u(\alpha,\beta_1,\beta_2,\varepsilon^2,z) = u(\alpha,\beta_1,\beta_2,0,z)$$

$$-(\varepsilon^2/4\beta_2)\Big\{[1/3]u(\alpha + 4,\beta_1 + 2\beta_2,\beta_2,0,z) + [1/3 + \beta_2{}^2]u(\alpha + 2,\beta_1 - 2\beta_2,\beta_2,0,z)$$

$$-[1/3]u(\alpha + 4,\beta_1 - 2\beta_2,\beta_2,0,z) - [1/3 + \beta_2{}^2]u(\alpha + 2,\beta_1 + 2\beta_2,\beta_2,0,z)$$

$$- 4\beta_2{}^5 \frac{\partial}{\partial \beta_1} u(\alpha,\beta_1,\beta_2,0,z)\Big\} + \ldots . \qquad (A.2.6)$$

Writing

$$u_o = u(\alpha,\beta_1,\beta_2,0,z) = \int_C (s - \beta_2)^{a_-} (s + \beta_2)^{a_+} e^{-sz}\, ds\ , \qquad (A.2.7)$$

we can then express (A.2.6) as

$$u(\alpha,\beta_1,\beta_2,\varepsilon^2,z) = u(\alpha,\beta_1,\beta_2,0,z) + \varepsilon^2(\partial_{\varepsilon^2} u)\Big|_{\varepsilon^2=0} + \ldots$$

$$= u_o - \varepsilon^2 h(u_o)/4\beta_2 + \ldots , \qquad (A.2.8)$$

where $h(u_o)$ is a functional of u_o and denotes the term in braces in (A.2.6). That is, once the functions u_o (which are independent of the magnitude of ε^2) are known, the behavior of $u(\alpha,\beta_1,\beta_2,\varepsilon^2,z)$ can, at least in principle, be determined for any value of ε^2 provided the Taylor series expansion is valid.

For the Taylor series to be valid the functions u_o must be analytic functions of ε^2 in the neighborhood of $\varepsilon^2 = 0$. Furthermore, the coefficients in the Taylor series must be bounded for all values of z. The functions u_o are analytic functions of ε^2 only for the contours corresponding to the solutions B_o, B_j and $\tilde{B}_j$ because these solutions become solutions of the second order differential equation when $\varepsilon^2 = 0$. On the other hand, u_o integrated along the contours for B_o, B_j and $\tilde{B}_j$ can be singular for certain values of z and the coefficients of the Taylor series are not bounded as z approaches these points. In the problem treated here, for example, singularities in b_j and $\tilde{b}_j$ can occur at the point $z = 0$ for $\alpha \geq 1$. In this case the expansion in powers of ε^2 is valid only for z bounded away from the origin, i.e., $|z| > |z_o| > 0$, for a given z_o, and for arg z restricted to the appropriate sectors, as given in the text by (4.15).

Figure Captions

Figure 1. Contours corresponding to solutions of (1.3) must proceed to infinity in the shaded open sectors labeled 1, 2 or 3. The integration plane is cut along the real axis from β_2 to positive infinity and from $-\beta_2$ to negative infinity. The plane of the paper represents the principal sheet with m = 0, n = 0 in (2.16).

Figure 2. The contours for the solutions A_1, A_2 and A_3 begin and end at infinity. The contour for the solution A_2 passes onto the adjacent Riemann sheet with m = 1, n = 0 in (2.16) when crossing the branch cut.

Figure 3(a). The contours for the solutions B_0 and B_j have at least one end point at $s = -\beta_2$. Contours that cross the branch cut pass onto the adjacent Riemann sheet on which m = 0 and n = 1 in (2.16) and are shown dashed. The contour for the solution $B_3(0,1)$ starts on the sheet (0,1) and crosses onto the principal sheet.

Figure 3(b). The same as Fig. 3(a) but for the contours corresponding to the solutions $\tilde{B}_j$.

Figure 4. Contours for all of the solutions shown in Figs. 2 and 3 are combined to facilate the derivation of the relations (2.18)-(2.23).

Figure 5. The position of the saddle point used to obtain an asymptotic representation for the solutions A_j is shown as a function of $\theta = \arg(\eta)$. The saddle point starts just above the right hand branch cut for $\theta = -\pi$ and traces out a circular path, crossing onto the adjacent m = 1, n = 0 Riemann sheet to end just below the branch cut at $\theta = 3\pi$. The contour for the solution A_1 lies in the (1,0) Riemann sheet.

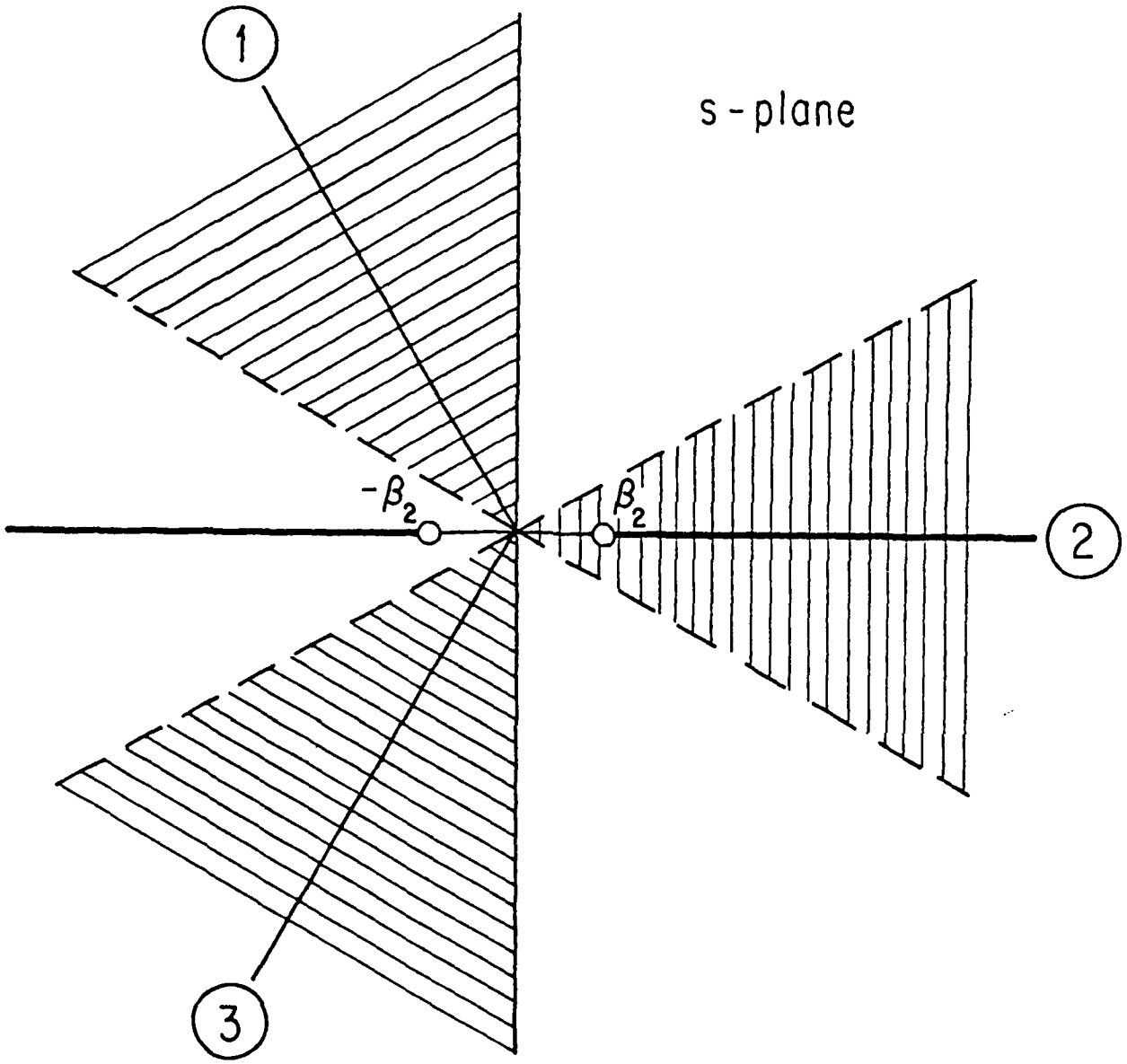

Fig. 1

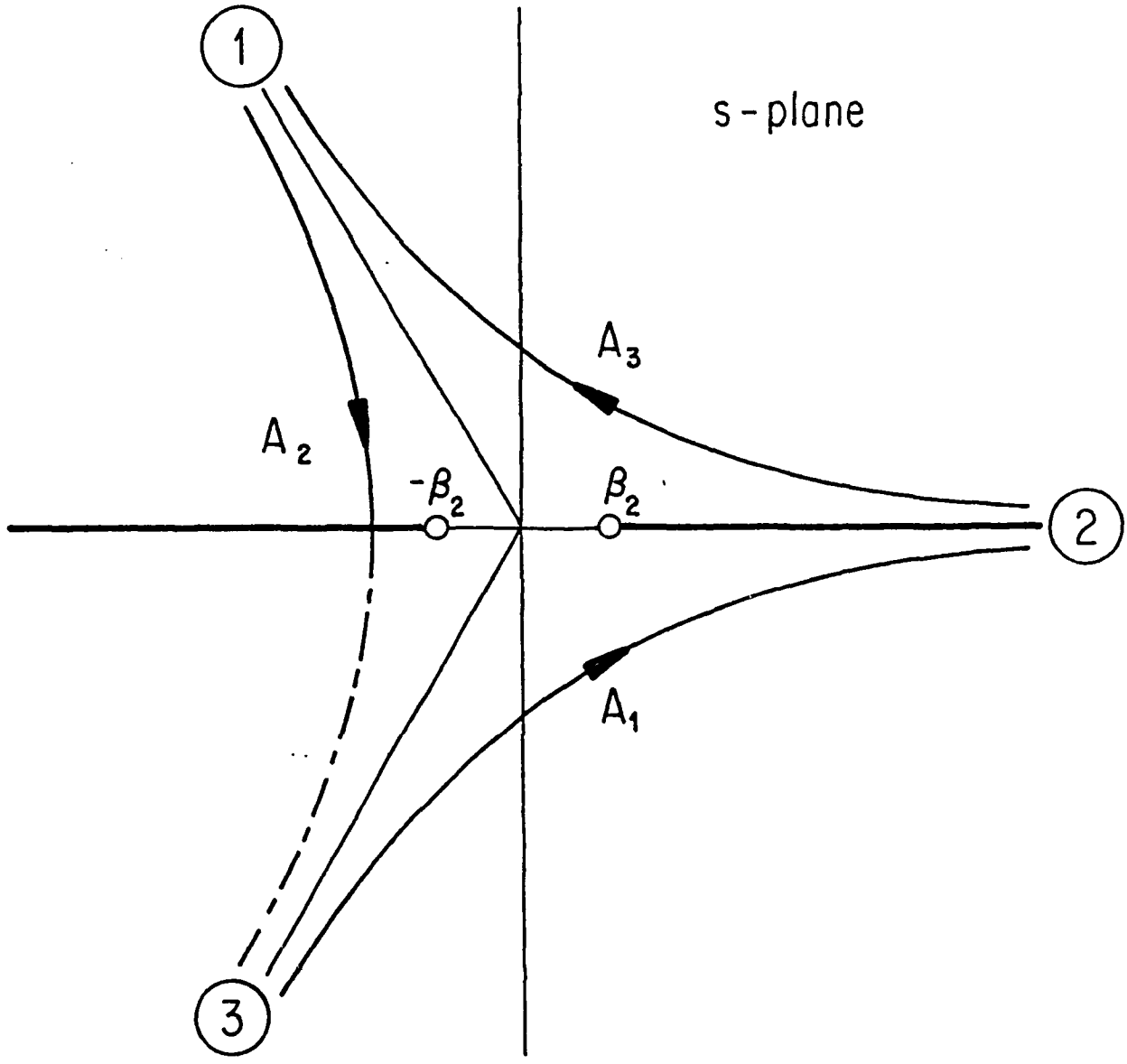

Fig. 2

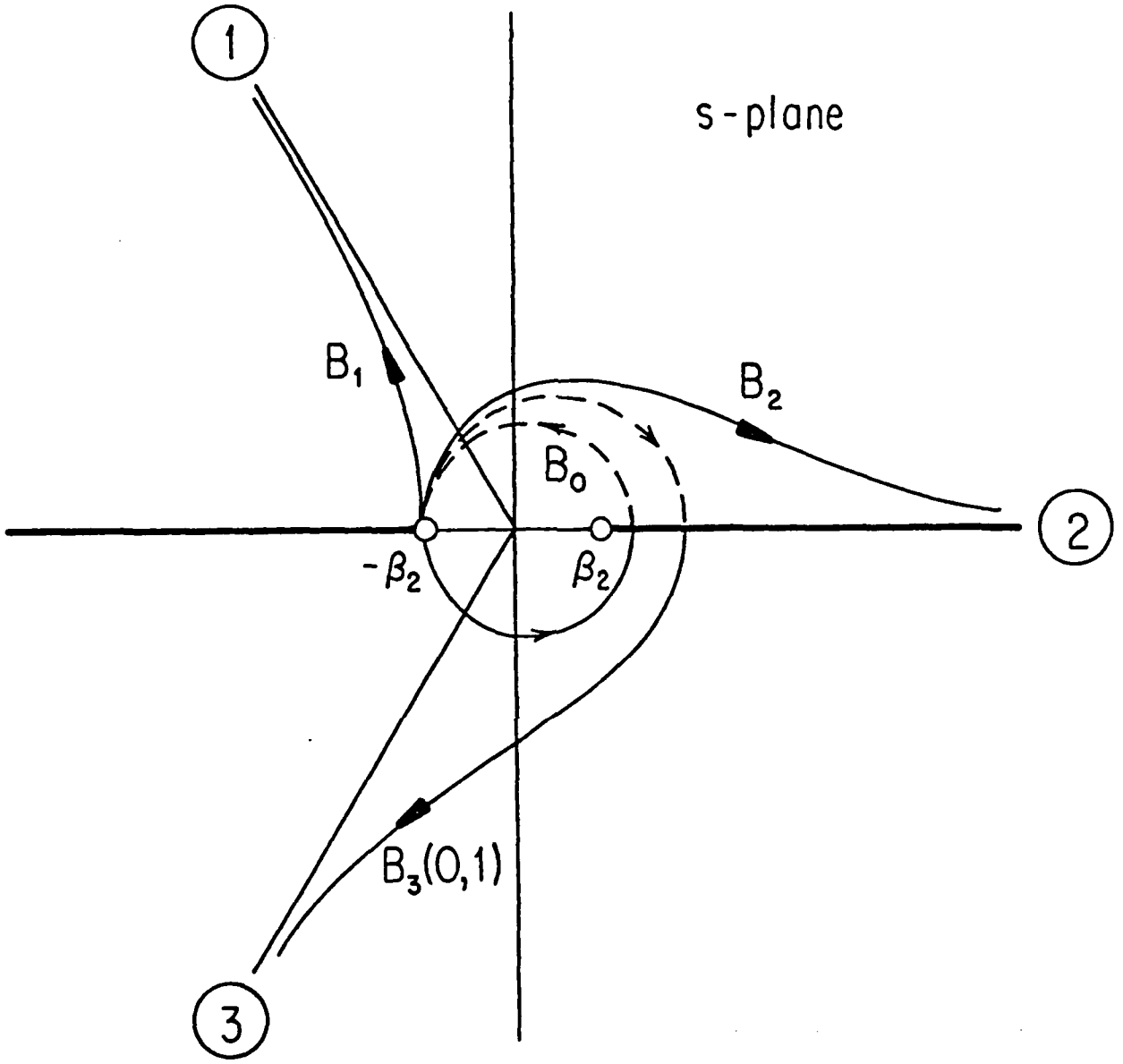

Fig. 3(a)

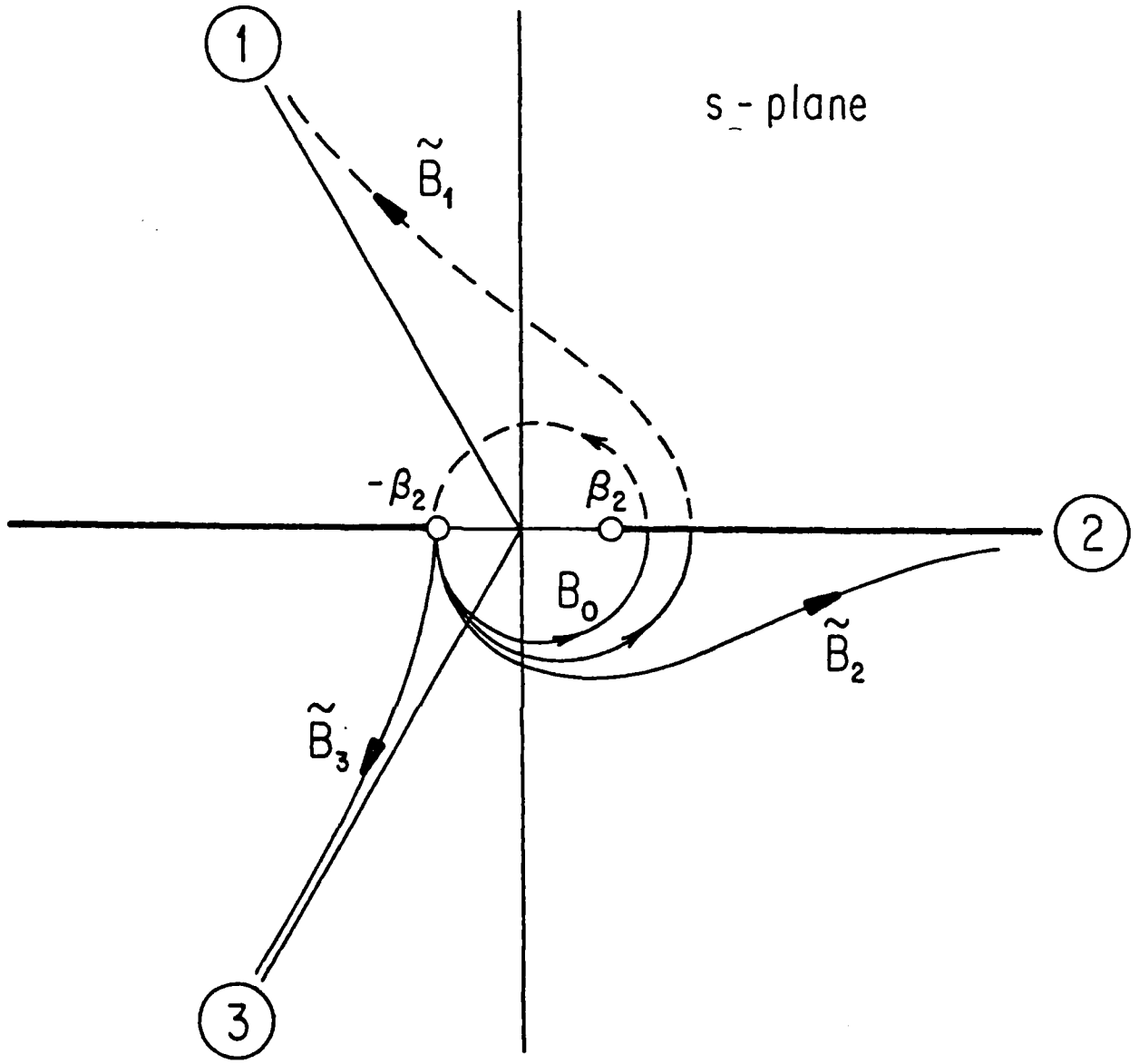

Fig. 3(b)

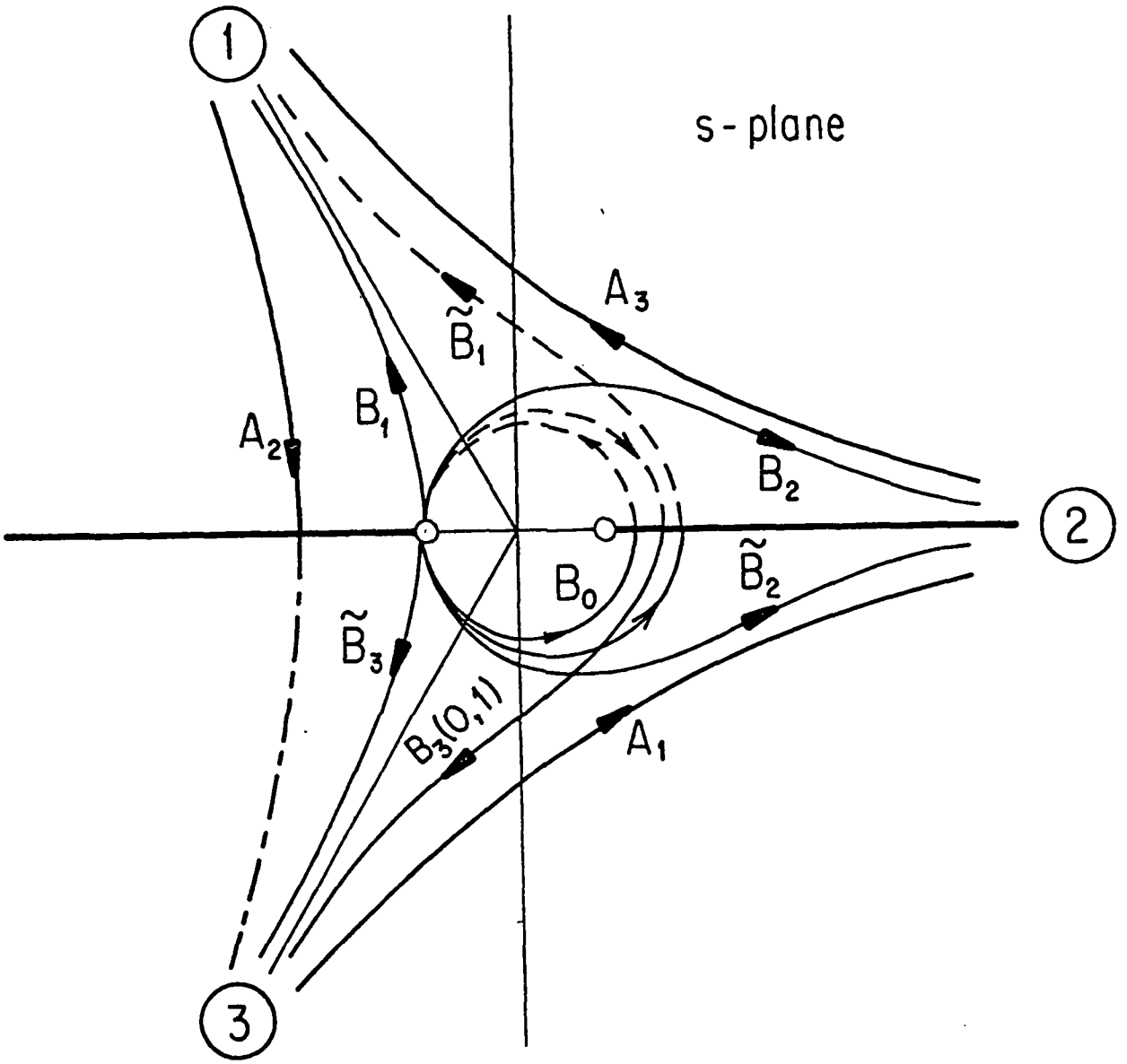

Fig. 4

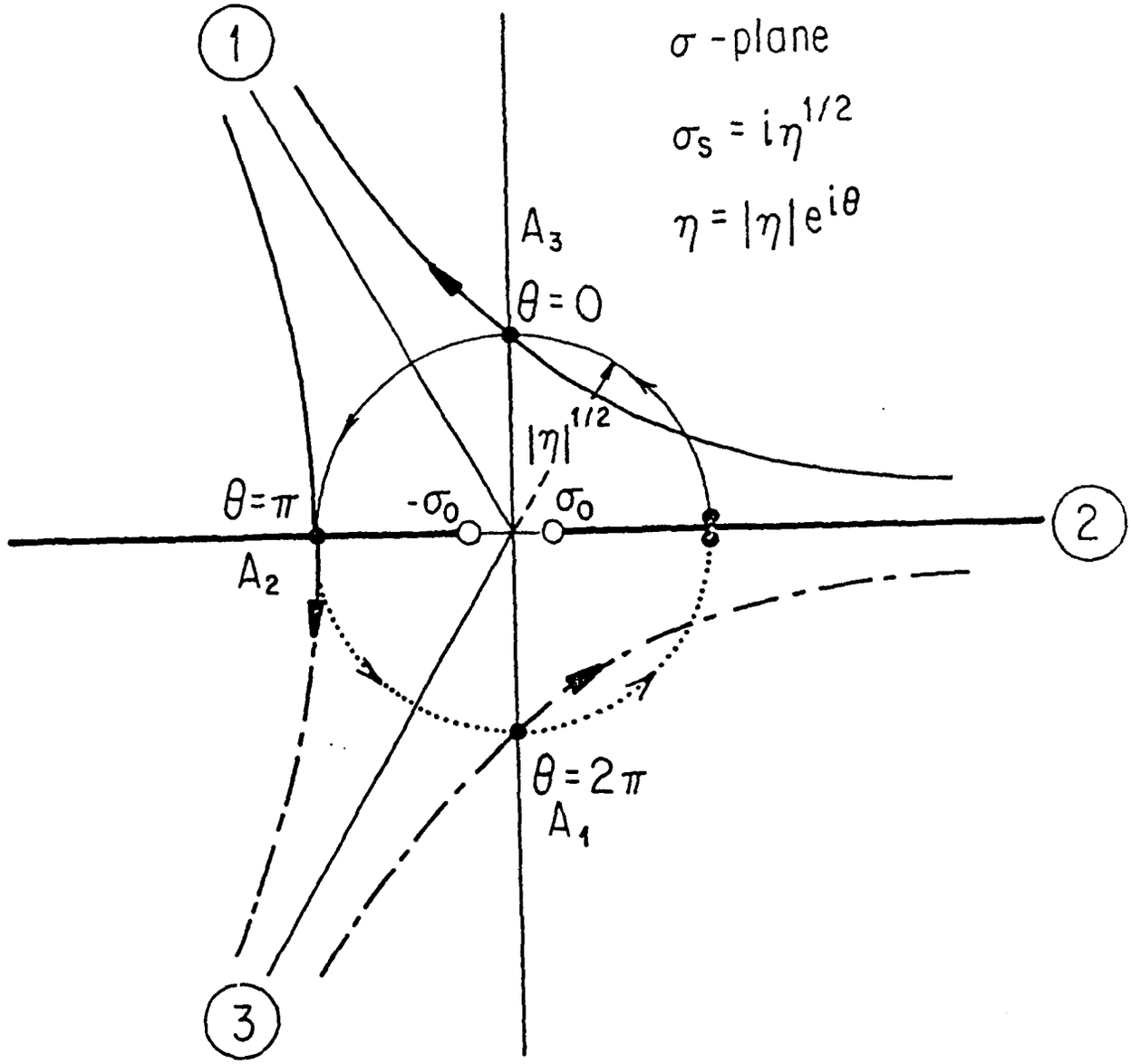
1
σ -plane
$\sigma_s = i\eta^{1/2}$
$\eta = |\eta| e^{i\theta}$
A_3
$\theta = 0$
$|\eta|^{1/2}$
$\theta = \pi$
$-\sigma_0$
σ_0
2
A_2
$\theta = 2\pi$
A_1
3

Fig. 5

PPG-688 "Observations of Odd-Half Cyclotron Harmonic Emissions in a Shell-Maxwellian Laboratory Plasma," J. M. Urrutia and R. L. Stenzel, March, 1983. To be submitted to JGR.

PPG-689 "Plasma Parameters, Fluctuations and Kinetics in a Magnetic Field Line Reconnection Experiment," N. Wild, March, 1983.

PPG-690 "A Plasma Wave Accelerator - Surfatron I and II," T. Katsouleas, J. M. Dawson, W. Mori, and C. Joshi, March, 1983/

PPG-691 "Electromagnetic Radiation and Nonlinear Energy Flow in a Beam Plasma System," David A. Whelan, March (1983)

PPG-692 "The Surfatron Laser-Plasma Accelerator", T. Katsouleas and J. M. Dawson, submitted to Phys. Rev. Lett. April, 1983

PPG-693 "The Reactor Physics of Startup Shutdown and Staged Power Operation in Tandem Mirror Reactors," R. Conn, F. Najmabadi, F. Kantrowitz, M. Firestone, D. Goebel, and T.K. Mau, April (1983).

PPG-694 "Transport and Ray Tracing Studies of ICRF-Heated Tokamak Reactors," T. K. Mau and R. W. Conn, April (1983).

PPG-695 "*Directional Velocity Analyzer for Measuring Eelctron Distribution Functions in Plasmas*", R. Stenzel, W. Gekelman, N. Wild, M. Urrutia and D. Whelan, April, 1983.

PPG-696 "Shape of the Magnetosphere", C. C. Wu, accepted for publication Geophys. Res. Lett., April, 1983

PPG-697 "Anomalous Transport by Magnetohydrodynamic Kelvin-Helmholtz Instabilities in the Solar Wind-Magnetosphere Interaction", A. Miura, submitted to Jour. Geo. Res., April 1983

PPG-698 "Helium Effects on Solids - a Reference Manual", N. Ghoniem and P. Maziasz, April 1983.

PPG-699 "Global Inelastic Structural Analysis of the Mars Tandem Mirror Blanket Tubes Including Radiation Effects", J. P. Blanchard and N. Ghoniem, April 1983.

PPG-700 "Self-Modulation Formation of Pulsar Microstructures" by A.C.-L. Chian and C. F. Kennel, to be submitted to Astrophysics and Space Science, May 1983.

PPG-701 "Evolution from Coherence to Turbulence in Plasmas," A. Y. Wong, P. Cheung, and T. Tanikawa, submitted to Proceedings in Inter-science Series on Statistical Physics, May 1983.

PPG-702 "Trapping of Plasma Waves in Cavitons", T. Tanikawa, A. Y. Wong and D. L. Eggleston, submitted to Phys. Fluids, May 1983.

PPG-703 "Instrumentation for Magnetically Confined Fusion Plasma Diagnostics", N.C. Luhmann Jr. and W. A. Peebles, invited review for Review of Scientific Instruments, May 1983.

PPG-704 "Velocity Redistribution in Lower Hybrid Current Drive," V. K. Decyk, G. J. Morales, J. M. Dawson, May (1983).

PPG-705

PPG-706 "MHD waves and Energetic Particles Associated with a Quasi-parallel Interplanetary Shock" by C. F. Kennel, C. R. Russel, M. Mellot, F. Scarf, F. V. Coroniti, K. T. Wenzel, T. R. Senerson, P. VanNes, J. Scudder, G. K. Parks, E. J. Smith, W. C. Feldman, to be published in Jour. Geophys. Research, May 1983

PPG-707 "Implementing the Absorbing Boundary Condition in Bounded Electromagnetic Particle Simulations", S. T. Ratliff and J. M. Dawson, May 1983

PPG-708 "Description of One Dimensional Electrostatic Particle Simulation Code BEPS1," V. K. Decyk, December, 1982.

PPG-709 "Linear Relativistic Gyrokinetic Equation", R.G. Littlejohn, May 1983

PPG-710 "On the relationship between Collisionless Shock Structure and Energetic Particle Acceleration," C. F. Kennel, May 1983, to be pub. in Proc. of Spring College on Radiation in Plasmas, IAEA, Trieste, May 1983

PPG-711 "Ponderomotive Effects in Nonneutral Plasmas", B. M. Lamb and G. J. Morales, submitted to Physics of Fluids, May 1983

PPG-712 "Stability of the Low-Frequency Hot Electron Interchange Mode for an EBT Model", Y. Ohsawa, J. M. Dawson and J. W. Van Dam, submitted to Physics of Fluids, May, 1983.

PPG-713 "Stability to the High-Frequency Hot Electron Interchange Mode", Y. Ohsawa and J. M. Dawson, submitted to Physical Rev. Lett., May 1983

PPG-714 "Simulation of Bumpy Torus with Hot Ion Rings", Y. Ohsawa and J. M. Dawson, submitted to Physics of Fluids, June, 1983

PPG-715 "Simulation of Bumpy Torus with Hot Ion Rings", Y. Ohsawa and J. M. Dawson, to be submitted to Phys. Fluids, June 1983

PPG-716 "Fourier Analysis of Polar Cap Electric Field and Current Distributions", by D. D. Barbosa, submitted to J.G.R June 1983.

PPG-717 "Enhancement of High-Harmonic Gyrotron Gain by a Dielectric Rod", D. McDermott, D. S. Furuno, and N. C. Luhmann Jr., submitted to J.I.M.W., June, 1983

PPG-718 "Non-linear Interactions During Magnetic Field Line Reconnection in Plasmas", R. L. Stenzel, and W. Gekelman, to be published in Physica D., June 1983


FILM